DEPARTMENT OF TECHNOLOGY AND BUILT ENVIRONMENT

Design and development of a multiband loop antenna for cellular mobile handsets

Amna Ikram

June 2010

Master's Thesis in Electronics/Telecommunications

Master's Thesis in Electronics/Telecommunications
Examiner: Prof. Claes Beckman
Supervisor: Dr. Stefan Irmscher and Johan Bäckman (Laird Technologies AB Sweden)

To My Parents

God has blessed me with wonderful parents who have always given me support and encouragement throughout their lives.

ABSTRACT

In this current age of advancements, the wireless products have been driven to small size while accepting the challenge of fulfilling the system requirements. This has become even more critical with respect to multiband functionality, which is an indispensable feature of modern mobile phones.

Antennas are one of the vital devices that enable wireless products. A good antenna design can relax the system requirements and improve the overall system performance. Hence, the field of designing handsets antennas is becoming interesting as the requirement to cover multibands is increasing with limitations of volume and required efficiency.

Within the scope of the work a cellular handset antenna has been studied and designed. Recent studies have also shown that the loop antennas are promising candidates for multiband operation in the mobile phones [1, 2, 17, 18, 24, 27 & 28].

The meander line loop antenna is investigated regarding its potential of covering today's GSM/UMTS bands in combination with the new bands for the upcoming LTE standard. The electrical length of the antenna is increased by folding and bending the structure in a definite order to get multimode resonant frequencies [2].

The simulations are done in Ansoft HFSS and CST Microwave Studio (MWS). The proposed antenna can passively cover 824-960MHz, 1710- 2170MHz and 2500-2690MHz. Furthermore, the potential impedance bandwidth is sufficient to also enable the coverage of the lower LTE bands 700-790 MHz by means of switching.

The benefit of this antenna that has been designed under the constraint of fitting into the limited available volume of a modern cell phone is its reduced dependency on system ground while retaining wideband impedance bandwidth and high radiation efficiency. It has shown very promising results for Hearing Aid Compatibility (HAC) and Specific absorption rate (SAR).

PREFACE

This thesis is submitted in partial fulfillment of the requirements for the degree of Master of Science in Electronics/Telecommunications Engineering at University of Gävle, Gävle, Sweden.

The thesis work has been conducted at the department of Advanced Technology, Laird Technologies AB, Kista during the period of February 2010 to May 2010.

The work has been supervised by Stefan Irmscher (Senior Staff Engineer) and Johan Bäckman (Manager). The examiner for the thesis is Professor Claes Beckman of ITB/Electronics department, University of Gävle.

Laird Technologies has provided the student licenses for Ansoft HFSS and CST Microwave Studio for the simulation work. The prototype fabrication is done at RF lab of the company.

Satimo Chambers are used for efficiency measurements. For HAC and SAR measurements Dosimetric Assessment System (DASY4) equipment is used. All these testing platforms are provided by Laird Technologies.

ACKNOWLEDGEMENTS

I am thankful to Johan Bäckman and Stefan Irmscher for believing in me and taking me into their advanced research group as a member, providing me an opportunity to work in a professional working environment.

Stefan Irmscher, my supervisor, without his support, constant supervision and strong technical guidance it would not have been possible to achieve my goals. His valuable suggestions, involvement in my work and friendly attitude has made this work possible.

Johan Bäckman, my manager, has been very helpful throughout my work. At every stage his strong encouragement has given me a lot of confidence. It's been a wonderful professional and personal experience to work with him.

I wish to express my warm and sincere thanks to all the group members of Advanced technology department, their extensive discussion around my work has been also of great value to my work. I would like to thank Beyhan Kochali and Jari Heinonen for being so helpful and providing me an opportunity to do testing at their measurement facilities.

My special thanks to Professor Claes Beckman, who has always given me his full support, encouragement and has accepted the responsibilities as an examiner for this thesis work. I would like to thank my all teachers and the staff at ITB/Electronics, University of Gävle for their support during my span of studies. I want to thank Peter Slättman for providing a student license for Ansoft HFSS.

A deep thanks to all my friends at Gävle and Stockholm, their company has made my stay in Sweden as a worth experience of my life.

At last I owe loving thanks to my sister Anila Asif, her constant support and prayers are ultimate success in my life, to my brothers, who are always guiding me throughout my stay in Sweden.

TABLE OF CONTENTS

LIST OF FIGURES

LIST OF TABLES

LIST OF ABBREVIATIONS

CST MWS: CST Microwave Studio
DASY: Dosimetric Assessment System
DCS: Digital Cellular System
E field: Electric field
EDA: Electronic Design Automation
FS: Free Space
FEM: Finite Element Electromagnetic
H field: Magnetic field
GSM: Global System Mobile communication
HAC: Hearing Aid Compatibility
HFSS: High Frequency Structure Simulator
LTE: Long Term Evolution
PCB: Printed Circuit Board
PCS: Personal Communication Service
PIFA: Planar Inverted F Antenna
RF: Radio Frequency
SAR: Specific Absorption rate
UMTS: Universal Mobile Telecommunications System
VOIP: Voice Over IP
WCDMA: Wide band Code Division Multiple Access
WiMAX: World Interoperability for Microwave Access

CHAPTER NO: 1 INTRODUCTION

1.1 Background

A single handset has to deal with the multiple services such as voice, data, video, broadcasting, and digital multimedia contents. The very often required bands are the global system for mobile communication GSM850, GSM900/1800, the digital cellular system (DCS) and the personal communication service (PCS) band. In addition to this, there is GPS and Bluetooth at 1.5GHz and 2.4GHz respectively.

Initially the mobile phones were mainly used for voice data using GSM900, later on GSM1800 and GSM 1900 were evolved in US for better network capacity, making a single resonance antenna to dual resonance. With the successful implementation of UMTS/WCDMA the dual band antenna has been changed to pentaband antenna.

The latest development is the LTE technology. This technology gives higher data rates for VOIP and online gaming requirements in the handsets and mobile internet devices. One foreseen associated problem with its antenna design is to cover LTE US 700MHz band while still covering GSM 900, GSM 1800, DCS, UMTS, PCS, and LTE EU 2500.

In the world of cellular communications there is an ever increasing demand of having light, short, slim handsets with low power consumption. With the rapid progress in the mobile phone market, a size reduction of mobile handset has been seen. The slimmer the handset, the more advanced and latest it is considered.

It has been proved from so far research that there are some fundamental limits and trade-offs between the physical size of an antenna and its gain, efficiency and bandwidth [3].

So one has to make some kind of compromise among volume, impedance bandwidth and radiation characteristics of an antenna while making the smallest possible antenna that can still work for a given application.

1.2 Development of various handset antennas

Looking at the history of handset antennas, different types of antennas such as whip, monopoles, diploes, PIFA, loop and helix have been used. One can start from the wire antennas such as monopole, see Fig.1.1. Its easy to design, light weight, and has omni-directional radiation pattern. However, the physical length of a monopole antenna is a quarter of the wavelength at the operating frequency making it impractically long when sticking out from the mobile phone. It has therefore been used as an external antenna.

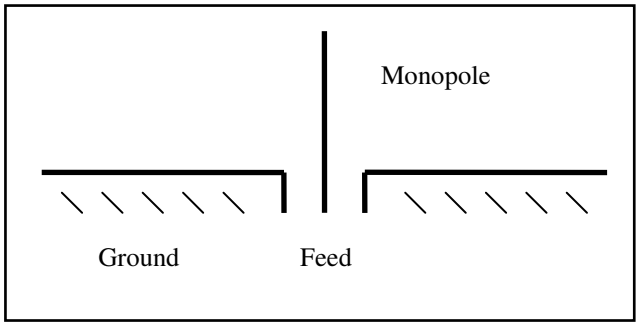

Fig.1.1. A typical monopole over a ground plane [4].

Another promising antenna that has come to replace the external monopole is the inverted- L antenna (ILA), see Fig.1.2. It has also a quite simple structure like that of the monopole, however, the input impedance has low resistance and high reactance like that of monopole [4]. Compensating for these shortcomings leads to the inverted-F antenna (IFA). Such a design adds a second inverted-L section to the end of an ILA, see Fig.1.3. This additional inverted-L segment makes it possible to tune the antenna. Both ILA and IFA have inherently narrow bandwidths. In order to improve the bandwidth characteristics, antenna designers have transformed the horizontal element from a wire to a plate resulting in the so called planar inverted-F antenna (PIFA), c.f Fig.1.4.

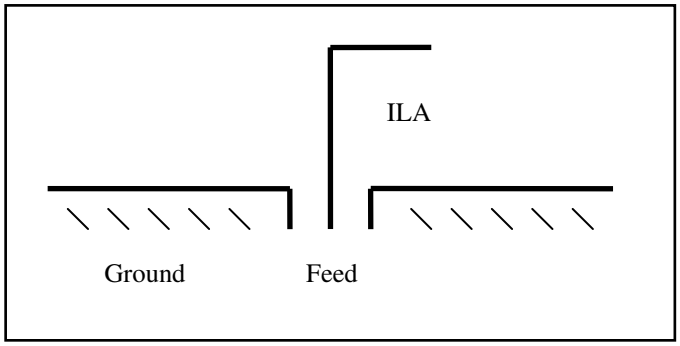

Fig.1.2. A typical ILA over a ground plane [4].

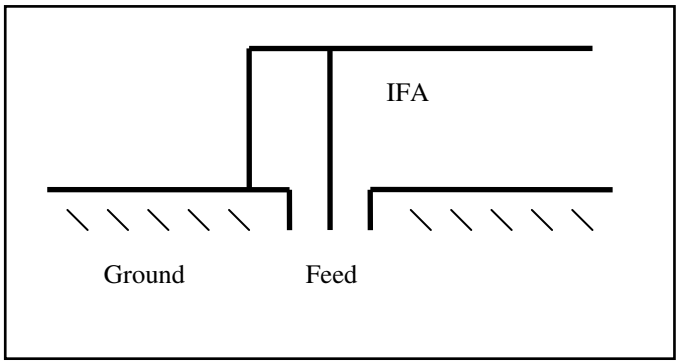

Fig.1.3. A typical IFA over a ground plane [4].

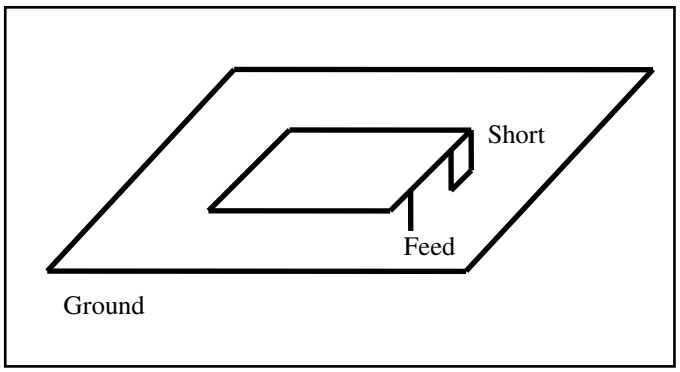

Fig.1.4. A typical PIFA over a ground plane [4].

Nowadays, the PIFA is widely used in mobile handheld devices. It has a self-resonating structure with purely resistive impedance at the frequency of operation. ILA, IFA and PIFA have quite simple structure. The tuning parameters to change the electrical performance are the height of the antenna with respect to the ground plane, path length of the resonator and the distance between the feed point and short point [3]. One of the limitations of PIFA over other antennas, such as monopoles or helices, which are placed outside the handset, is the less gain.

The handset antenna designs starting from a monopole to the PIFA indicates that the essential component of a handset antenna is ofcourse “wire”. The patch(s) slot(s), and stub(s) are only used to compensate for the mismatch and improve the radiation characteristics [4].

Usually PIFA elements have narrow bandwidth but many interesting designs are successfully covering multiband requirements. Multiple resonances can be achieved by making different multicurrent paths, multilayer structures and slits [4]. The usual antenna height for the PIFA is 5-10mm.

1.3 Objective

The main objective of this work is to do a concept study of loop antennas. To see the bandwidth potential of covering LTE band along with required penta bands. Its current distributions, dependency on ground plane and body effect on antenna tuning, also looking into the HAC mode and its compliance with SAR standards. A detailed discussion about HAC and SAR can be seen in Chapter 4 and 5.

Nowadays it is highly demanding that with multiband performance, the antenna structure has to remain compact and its over all volume should not go beyond the acceptable range. The normal techniques to reduce the size of the antenna are to use shorting pins, stubs, reactive loading and meandering, or folding the resonating antenna sections in a compact configuration. [5].

Typical smart handset antenna geometry of $50*10*5mm^3$ has been proposed and a meanderline loop antenna is designed meeting the required bands of LTE US 700MHz, GSM 900, GSM 1800, DCS, UMTS, PCS, and LTE EU 2500.

Different kinds of loop antenna designs have been proposed in the past. In the research papers, some are giving information about the coverage of multiple bands and some of them give idea about the performance for efficiency, SAR or HAC at a certain frequency. The proposed work in this thesis contains all the information together, comprising of antenna design, its usage for multiple bands along with its performance for efficiency, SAR and HAC for all the bands. As far as the research studies are concerned, that have been done during the span of this thesis, no such paper has been seen which explains everything together and which covers all these bands within the same geometry and with very good performance for SAR and HAC.

As the antenna has to cover the lower band of 700MHz and higher band of 2500MHz, folded and meandered loop antenna has been suggested for multiband operation. The proposed antenna consists of a radiating element of the folded loop structure with uniform meandering on the top side of radiator and unsymmetrical at the back side. One end is attached to the feed and other end is connected to ground plane. The feeding and shorting locations are at the center of the lower antenna side in order to make the current distributions symmetrical on the printed circuit board (PCB).

The antenna has balanced and unbalanced modes for certain frequencies. In the balanced or self balanced mode it results very less currents on the ground plane, which makes it appropriate for HAC standard. The proposed antenna may be very effective in mitigating its performance degradation due to the body effect because it has lower surface current density on system ground plane as compared to the conventional PIFA antennas. Which depends on ground plane for their radiation characteristics, hence the dependence of the loop antenna performances on the system ground plane can be relaxed.

1.4 Thesis Organization

This report has been divided in the following order. Chapter 1 contains the background for the mobile antennas, requirements of being used for multiple applications and objective for this work. Chapter 2 contains the typical challenges faced by small antennas in terms of its bandwidth, efficiency and quality, theoretical explanation for balanced and unbalanced antennas and dependency on system ground plane. Chapter 3 explains the concept study for a loop antenna, the proposed design simulations in HFSS and measured results for the fabricated prototype. Chapter 4 and 5 gives the theory for the SAR and HAC standards, respectively, simulations in CST MWS with some comparison with prototype measured results. Chapter 6 contains a comparison between loop and PIFA antennas and advantages achieved by former over the later. Some conclusions drawn from this work and future work is also presented.

CHAPTER: 2 SMALL ANTENNA THEORY AND BACKGROUND

2.1 Challenges in mobile antennas

Mobile device communications have become an important part of the telecommunication industry. Starting with the paging services, there are new applications emerging every day including tagging, wireless computer links, wireless microphones, remote control, wireless multimedia links, satellite mobile phones, wireless internet so its just about everything “goes mobile”.

The significance of mobile phones has increased rapidly in last few years, it has become a necessity to a human life. Moreover, the rapid growth in mobile communication systems has led to a great demand for the development of internal antennas with the multiband and broadband operations.

Handset platforms can have different designs like bar, clamshell, slider, swing and flip. In the case of a clamshell, slider and flip, the connection points for two parts can have influence on the antenna performance [6]. There is a need to make a self resonant and self immune antenna, as there might be some impact on antenna performance because of the style and its geometry and the presence of other antennas for GPS or for MIMO functionality. It has lead to an increase in the complexity of the antenna along with the commercial pressures to make cheaper models that occupy less volume in the handset.

The two big challenges in designing a handset antenna are: how to use a single antenna to cover all the useful frequency bands and then how to make the antenna size small enough so that multiple antennas can be deployed in a handset. So one can see the pressure to design small, lightweight and user friendly mobile handsets devices creating a need for the optimal antennas for mobile applications.

The antenna is a device which is used to transform a guided wave to a radiated wave or the other way around. According to the wave propagation theory the radiation capability of an antenna depends on its wavelength for the designed frequency. So the size of an antenna is much more important in determining how well and for which

frequencies this transformation will be satisfactory. For an efficient antenna the size should be of the order of half a wavelength or larger. By miniaturizing the size of an antenna, it will influence its radiation characteristics, bandwidth, gain and efficiency. Moreover, it is not always easy to feed a small antenna efficiently.

Some discussion has been presented below to demonstrate the effect on efficiency (η), bandwidth (BW), and Quality factor (Q) of an antenna with respect to its size.

2.2 How to define a small antenna?

The first question that comes is how to define an antenna as a small antenna or a large antenna. There have been some theories that have suggested the size to be of some fractional part of λ (wavelength) as to mark the limitation. Wheeler has defined the limitation as λ/ π, while some other makes it λ/10, λ/8 or λ/4 [4].

The size of the antenna is very much influenced by the operating frequency in combination with the targets for bandwidth and efficiency. Electrically large antennas have higher efficiencies as compared to electrically small antennas. In the case of internal mobile phone antennas, the available volume is typically small with respect to the wavelengths of the lower cellular frequency bands (several hundreds of MHz). Therefore, it is important to understand the trade-offs involved to make a successful design.

Some of the techniques that have been extensively used in the mobile communication business, to make the design compact while fulfilling the requirements, are, loading the antenna with lumped elements, high dielectric materials or with the conductors using ground planes and short circuits, optimizing the geometry and using the antenna environment such as the casing to reinforce the radiation .

2.2.1 Dielectric Loading

Dielectric materials available today were originally designed for dielectric resonator filters putting stringent requirements on the material parameters. Thus, today's antenna designers can make use of available low losses and wide range permittivity (up to 100) materials [7].

Antennas can be loaded by a dielectric material. The permittivity and shape of the material determines the effective wavelength. As the wavelength is shorter in a high permittivity material, the antenna size can be reduced. This is due to the concentration of the electric field in high permittivity materials, which makes the adaptive launching of a guided wave into free space more difficult. High permittivity materials usually have higher dielectric losses. If the material is loss free, higher permittivity increases the Q-factor at a given frequency and thereby reduces the available bandwidth. The added losses, on the other hand, increases the bandwidth, but, on the expense of radiation efficiency.

Apart from size reduction, another reason to use dielectric antennas is that they are more resistant to detuning when placed to other objects like the human body in the case of the handset antennas. If the dielectric material is used in the antenna where the electric fields or currents are high, it makes the antenna more efficient than its all metal counterpart [7].

2.2.2 Lumped component matching

Antennas with a size smaller than half a wavelength show a strong reactive input impedance and very low resistance. This reactive impedance can be compensated by loading the antenna with lumped components. This might be a simple way to make the antenna smaller, at the lower resonant frequency.

This can be illustrated by the example of a simple loop. Its input impedance is highly inductive and can be matched with a capacitor. As the radiation resistance of a loop antenna is much small, any losses caused by the matching circuit or the antenna

structure itself can reduce the η. If there is less loss then it improves the Q, thus reducing the BW.

2.3 Resonant frequency

Another parameter associated to the antenna design is the frequency of operation or the resonant frequency. There is a range of frequencies over which the antenna can be operational, giving the bandwidth of an antenna.

The antenna can be considered as a tuned circuit containing inductance and capacitance. It has a resonant frequency at which the capacitive and inductive reactances cancel each other. At the resonance it has purely resistive impedance, which is a combination of loss resistance (Rloss) and radiation resistance (Rr). These capacitances and inductances of an antenna are determined by the physical geometry of the antenna and its environment.

2.4 Input Impedance of an antenna

Antenna impedance is defined as the real (R) and reactive part (X) seen at the port of the antenna. It is a function of frequency (ω). If no losses are included in the antenna model, then the real part impedance seen at the port is purely radiation resistance.

$$Z(\omega)=R(\omega)+jX(\omega)$$

2.5 Radiation resistance

The radiation resistance is a measure of the antennas ability to radiate an applied signal into space or to receive a signal from space. The radiation resistance is not a dissipative resistance, rather its a measure of the power radiated into the free space for a given input current [8].As the size of an antenna decreases, its reactance increases but its radiation resistance decreases. Thus, large antennas have higher radiation resistances and higher radiation efficiencies, given by following relationship.

.

$$\eta rad = \frac{Rr}{Rr + Rloss}$$

Where, Rloss is the resistance due to ohmic losses. The ηrad can be maximized by increasing the Rr, which ofcourse depends on the size of the antenna.

2.6 Quality Factor

The Q of an antenna is defined as the ratio of the power stored in the reactive field to the radiated power. It is used to describe the antenna as a resonator and quantifies the potential bandwidth of an antenna. Higher value means a sharp resonance and narrow bandwidth. It depends on the input impedance of an antenna as shown below.

.

$$Q = \frac{\text{AntennaReactance}}{\text{AntennaResistance}}$$

$$Q = \frac{w}{2 \cdot R(w)} \cdot \sqrt{R(w) + \left(X(w) + \frac{|X(w)|}{w} \right)^2}$$

To increase the antenna bandwidth, Q has to be reduced, which can be achieved by allowing the antenna to occupy more space. For the wire antenna, it can be achieved by bending the wires in an efficient way. In the theory there has not been any technique given to reduce the Q value. One possible way can be to add losses, which ofcourse adversely effects the η.

A fundamental theoretical limit for the minimum Q value of a small antenna is given by McLean [4], considering the antenna is inside a sphere of radius a

$$Q = \frac{1}{(k \cdot a)^3}$$

Where

$$k = \frac{2\pi}{\lambda}$$

2.7 Efficiency

Efficiency of an antenna can be divided into radiation efficiency which depends on the antenna structure or the radiation resistance, while the other is the total efficiency which includes the matching of an antenna to the power source or the return loss S11, where the expected value is usually -6dB.

$$\eta total = \eta rad \cdot \left[1 - \left(|S11| \right)^2 \right]$$

2.8 Bandwidth and Quality factor relation

In circuit theory, high Q is desired. While in antennas as large bandwidth is required, low Q value is required as

$$Q \alpha 1/BW$$

In small antennas the Q is high, as it has low radiation resistance and high reactance, which governs the low BW. This makes it difficult to match and predominant detuning from surroundings.

2.9 Concept of an unbalanced and balanced antenna

Consider a simple monopole structure, i.e., a single ended structure. The length of the antenna is a quarter of a wavelength. To make this antenna work more efficiently and have large bandwidth, image theory is used which makes the ground plane as a part of the antenna and improving the radiation characteristics. Such structures or antennas that are depending on the ground characteristics are known as unbalanced antenna, where PIFA is a good example.

The current towards the ground plane is not balanced in case of a monopole as compared to the balanced antennas and thus causing a radiation of electromagnetic field from the ground plane. For balanced (feed consists of two lines over ground) and self balanced (single feed, but still balanced ground currents) structures the ground plane does ideally not contribute to the radiation characteristics. A dipole antenna has

a balanced structure. Fig. 2.1 demonstrates the flow of currents towards the ground plane for both cases.

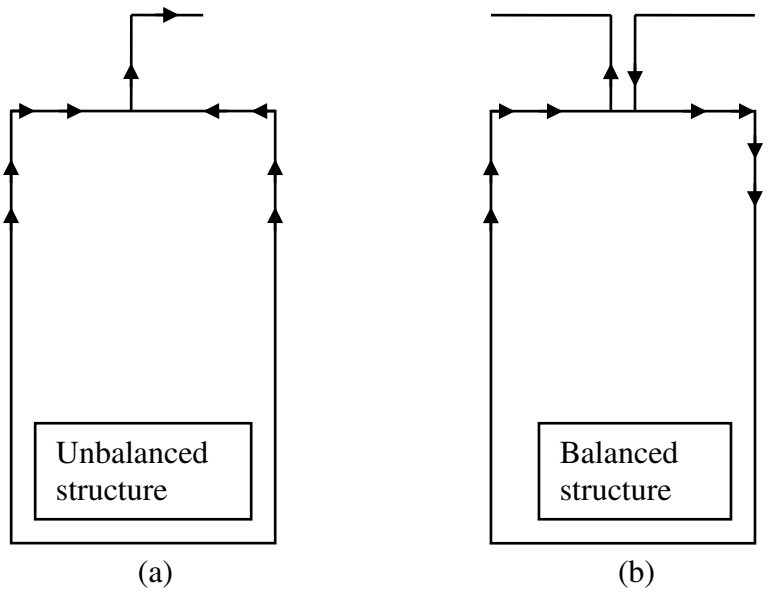

Fig.2.1. (a) a monopole antenna (b) a dipole antenna.

Fig.2.1 (a) shows currents towards antenna from the PCB, while in Fig.2.1 (b) two opposite currents on PCB can be seen, which cancel each other, making the antenna structure independently resonant.

PIFA antenna, as shown in Fig1.4, has an unbalanced structure. It is a popular internal multiband antenna. However, it suffers from poor efficiency and narrow bandwidth. PCB is added as an additional radiating element to the antenna, which improves the bandwidth.

It can be seen from the monopole current distribution that it will lead to large excited surface currents on the system ground plane. The location of the antenna near the end of the PCB is important for proper coupling or to excite the supporting wavemode on the chassis [10].This dependency then puts some limitations on the width and height of the antenna element with respect to the ground plane.

In the case of a balanced antenna which is more independent of the ground plane, it seems natural that when the ground plane conditions are changed, the radiation characteristics of the antenna will be less affected. The balanced structure offers the

advantage of reduced detuning and greater efficiency as compared to the single ended monopole antenna, when the mobile device is in normal use [11, 12].

To meet the same bandwidth requirements, usually the size of a balanced antenna is twice as large as an unbalanced antenna, e.g., a monopole (quarter wavelength) and a dipole (half wavelength).

In the low band of 900 MHz the antenna has to be unbalanced as the wavelength is in a region where the whole PCB is needed as the primary radiator. The size of the antenna is inside the Chu-Harrington limit [7], which means it will either be an inefficient radiator or lack sufficient bandwidth without the use of PCB as the main radiator. The balanced mode would typically be above 1.5GHz.

2.10 Chassis effect

The maximum length of mobile handsets is less than half a wavelength at 900 MHz and the dimension of the antenna element itself is clearly smaller. Thus, the structure can support only a few significant wave modes. The impedance bandwidth enhancement can be achieved in chassis wavemode, which can be optimized by designing the antenna element actually to work as a coupling element [10].

The fields and currents of this wavemode are concentrated in the vicinity of the small antenna element and for this mode the chassis acts as a ground plane with currents creating the mirror effect for the antenna element. The length of the handset chassis is clearly larger than the width, the structure supports single wire or thick dipole type current distributions.

From so far discussion it has been shown that the conventional antennas such as external stubby antennas and internal PIFAs are of unbalanced type and induce large currents that flow in the conductive surface of the chassis or PCB. Using such a mobile device, results in some absorption of the current flowing on the PCB to the body, making the efficiency lower and detuning the antenna.

Separating the radiation quality of the antenna from the chassis radiator is sometimes difficult. Because at lower frequency the PCB is a main radiator while at higher frequency the antenna dimensions are large enough to become an efficient radiator.

It can be concluded that when the total bandwidth achieved by the antenna and chassis is less, it is assumed to represent the case where the contribution of the chassis radiation is small and when the maximum bandwidth is obtained, it is the case when both antenna and chassis resonates together [13].

CHAPTER: 3 DESIGN AND SIMULATION OF MEANDERED LINE LOOP ANTENNA

This chapter contains concept study about loop antennas, design methodology, discussion about used softwares, simulated and measured results.

3.1 Loop Antenna

The revolution in wireless industry has dramatically increased the higher data rates for voice and data, creating demands for smaller and better wireless terminals. The new performance demands needs multiband operation with higher radiation efficiency. The dual band antenna requirements have been changed to penta band antennas, while the covering frequency ranges from MHz to GHz, making a challenge for antenna designers to make state-of-art antennas. LTE is considered as 4G and requires higher data rates, two new bands have been assigned as LTE US 700MHz and LTE EU 2.6GHz.

Currently the design of antenna includes a main radiator operating at lower band (900MHz) and first higher band (1800 MHz). A shorted parasitic is added for second higher band resonance that occupies valuable space [14]. As the size of mobile phone is constantly shrinking, there is a need for an antenna, which covers all expected bands within a limited volume, and with good radiation efficiency.

Generally loop antennas have different shapes, circular, rectangular or elliptical. The radiation pattern depends on the shape of the loop. The size of the loop can be categorized as electrically small or large depending on the circumference of the loop. Circumferences of less than $\lambda/10$, and of the size of about λ are considered as small loops, and large loops, respectively [15]. A small loop has low radiation resistance, which is typically a problem associated with electrically small antennas.

The question is how to increase the electrical length of an antenna within small physical dimension. This could be done by bending, folding, creating slits in the paths or meandering [14]. Consider a simple patch antenna, the length of the patch defines the resonant frequency. It has a limited bandwidth but if some slit is created in the patch, another path is introduced in the patch and its bandwidth enhances [16].

Both loop and dipole are double ended structures and balanced especially for the higher frequency (one wavelength mode) as explained in Chapter 2.The currents in the ground plane are opposite in direction and hence do not much influence the antenna characteristics at that frequency. For lower frequencies, the required antenna size is small and there are unbalanced currents in the ground plane, which influence the antenna characteristics.

A folded and bent loop designed for a λ/2 path length, is resonant for λ/2, λ and 3λ/2. This multi resonant behaviour makes loop antenna, a potential candidate to cover multibands without occupying too much space [17, 18]. In Fig.3.1, three different modes are explained along with the current distributions on the antenna element and the ground plane. For a length of λ/2 and 3λ/2, one and three null current occurs, respectively, which makes the same direction of currents on the PCB. While for λ, two nulls occur, this gives opposite currents on the ground plane and thus reducing the free currents on the ground plane.

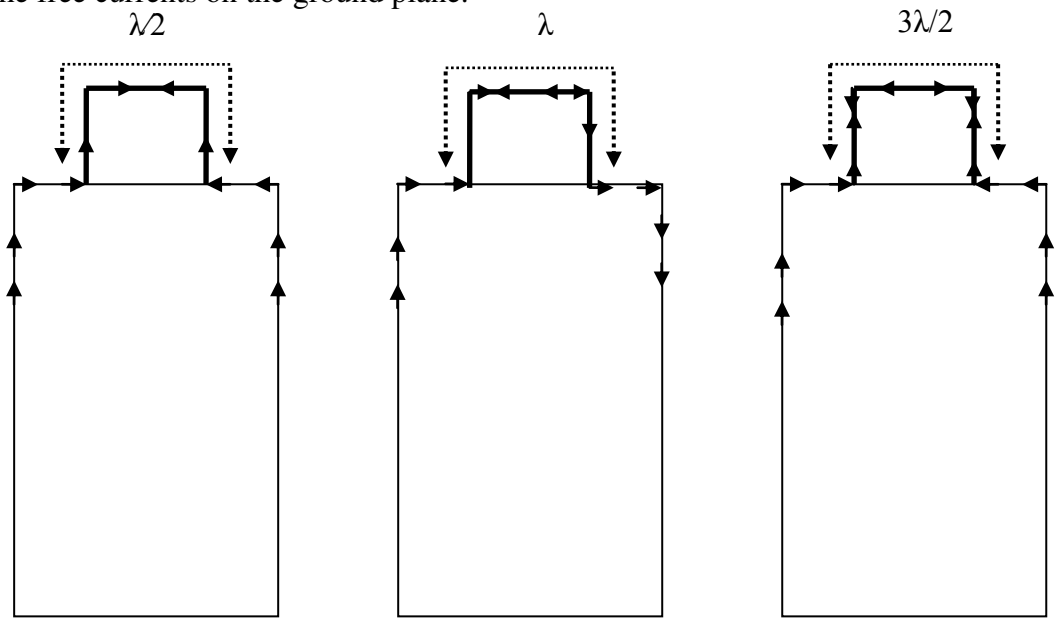

Fig.3.1 Current distribution on loop and ground plane for λ/2, λ and 3λ/2.

So the importance of balanced modes can be seen easily. The relaxation of the ground plane currents makes is better for the SAR and HAC to be discussed in Chapter 4 and 5, respectively. In the design task, the minimum frequency is 700MHz and the maximum resonant frequency is 2.6GHz. The free space wavelength λ for 750MHz is 400mm, so a structure of length 200mm can be implemented. A simple loop is not

enough to excite all the required modes and to cover the required bandwidths, so meandering is done as explained in section 3.4 and 3.5.

3.2 Simulation Tools

Ansoft HFSS and CST MWS are used for full wave analysis of the multiband antenna structure. HFSS performs complete FEM modeling of three dimensional passive linear microwave circuits, including radiating structures. This extremely powerful design tool is used for many types of components, especially antennas, antenna feed structure and other microwave passive components. HFSS uses discrete, fast, interpolating sweep types. Typically discrete sweep requires more memory to produce accurate results as compared fast sweep.

CST MWS has many options for the simulation. The transient solver is the most used solver, which can obtain the entire broadband frequency behavior of the simulated device from only one calculation run. It is very efficient for many RF frequency applications such as connectors, transmission lines, filters, antennas and many more. The transient solver becomes less efficient for low frequency problems where the structure is much smaller than the shortest wavelength. For such cases it can be advantageous to solve the problem by using the frequency domain solver. The latter approach is most efficient when only a few frequency points are of interest.

All the important parameters associated with the antenna design can easily be presented with the help of these software tools like the electric field, magnetic field, surface currents, radiation plots, return loss, gain, SAR and many more. In CST a build-in macro is used to simulate the HAC phenomenon.

3.3 Selected Geometry

A modern standard cell phone geometry is selected. The carrier volume is $50*10*5mm^3$. Permittivity ε_r is 2.66 and loss tangent $\tan\delta$ is 0.00629 @2.44GHz. Copper is used as a metal part of the antenna having conductivity of 5.8e7 S/m and thickness of 0.1mm. PCB length is taken as 100mm. A semi rigid cable is used to

feed the antenna from the backside. The radiating element is placed on both sides of the carrier to utilize the available area effectively.

3.4 Simple loop simulations

For the concept study some basic simulations are done to start with. A simple wire loop in free space is simulated. The model and impedance plot is shown in Fig.3.2 (a&b). A multiple resonant behaviour can easily be seen. Q is calculated from the formula given in Chapter2. Q value and percentage bandwidths for the different bands have been assigned, as can be seen from the Table3.1

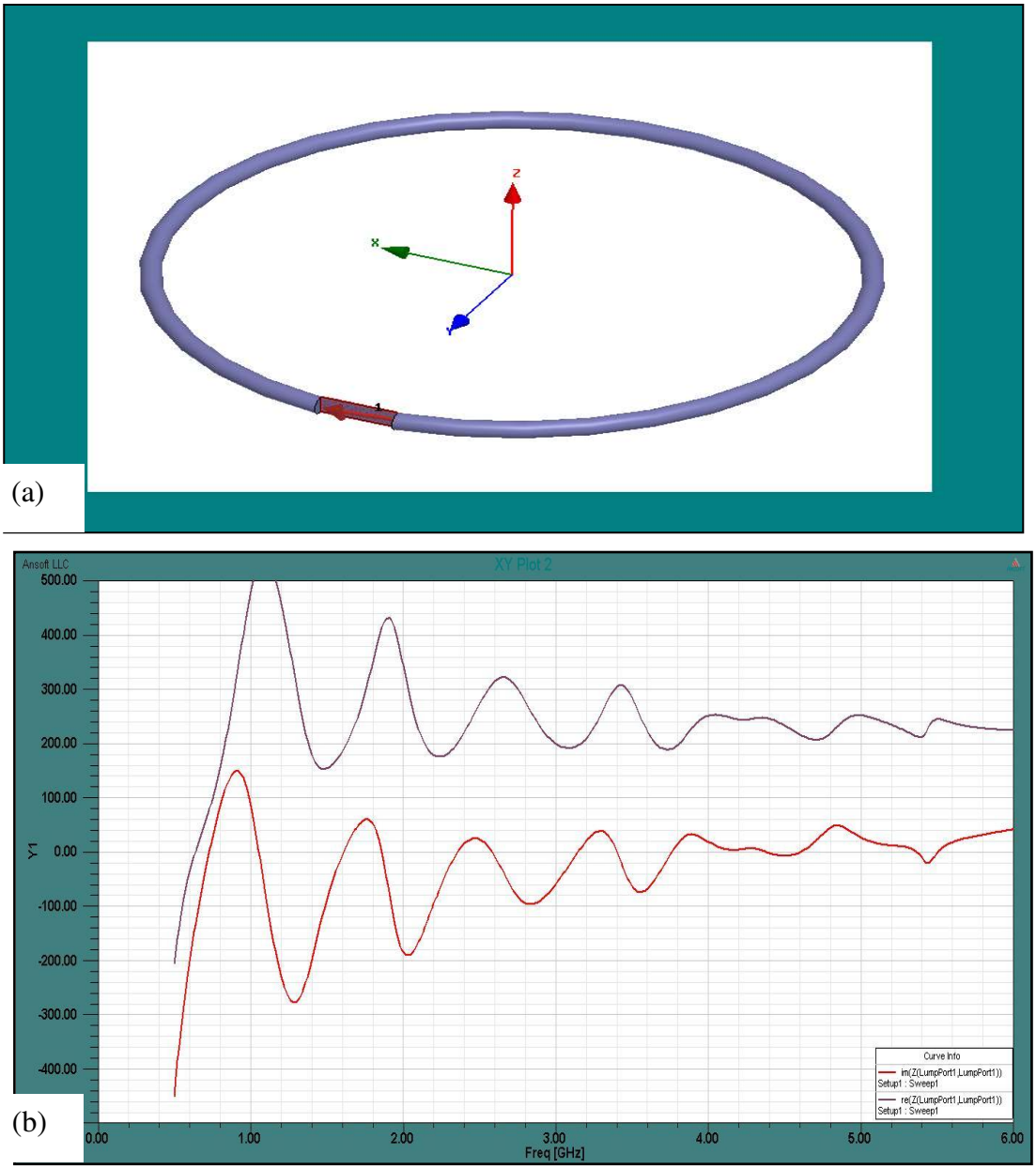

Fig.3.2 (a) A wire loop model in free space, (b) Impedance plot.

Start frequency fmin (MHz)	Stop frequency fmax (MHz)	Center frequency fo (MHz)	Bandwidth BW (MHz)	Percentage Bandwidth %	Quality factor (Q)
700	790	745	90	12	23
824	960	892	136	15.2	8.7
1710	2170	1940	460	23.7	5.6
2500	2690	2595	190	7.3	18.2

Table.3.1 Frequency list with the required percentage BW and Q.

The design has been started by folding the loop around the carrier.Fig.3.3 shows a simple and meander loop antenna models.

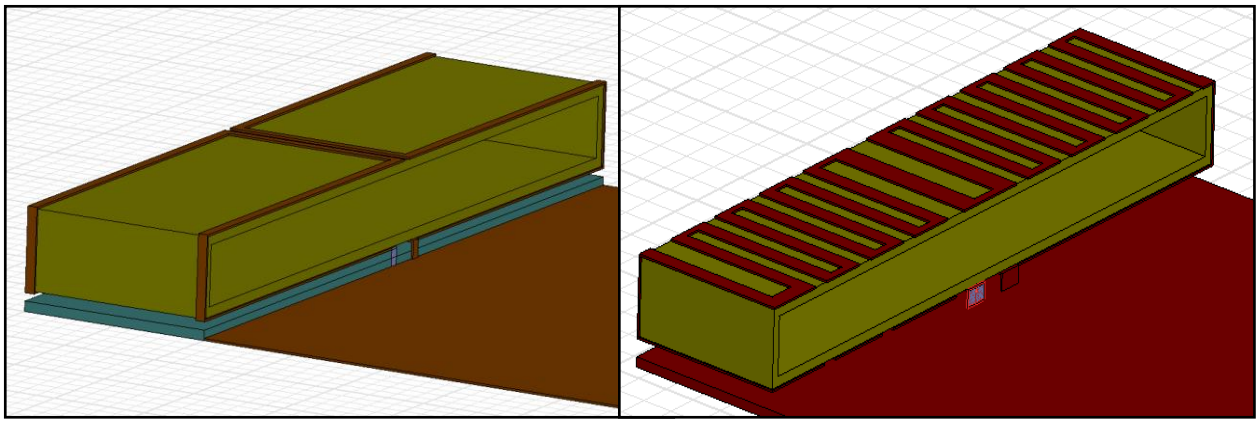

Fig.3.3. A simple loop and meander loop antenna model.

The S11 response c.f Fig.3.4 shows that by introducing the meandering a shift in the frequency and bandwidth enhancement can be seen.

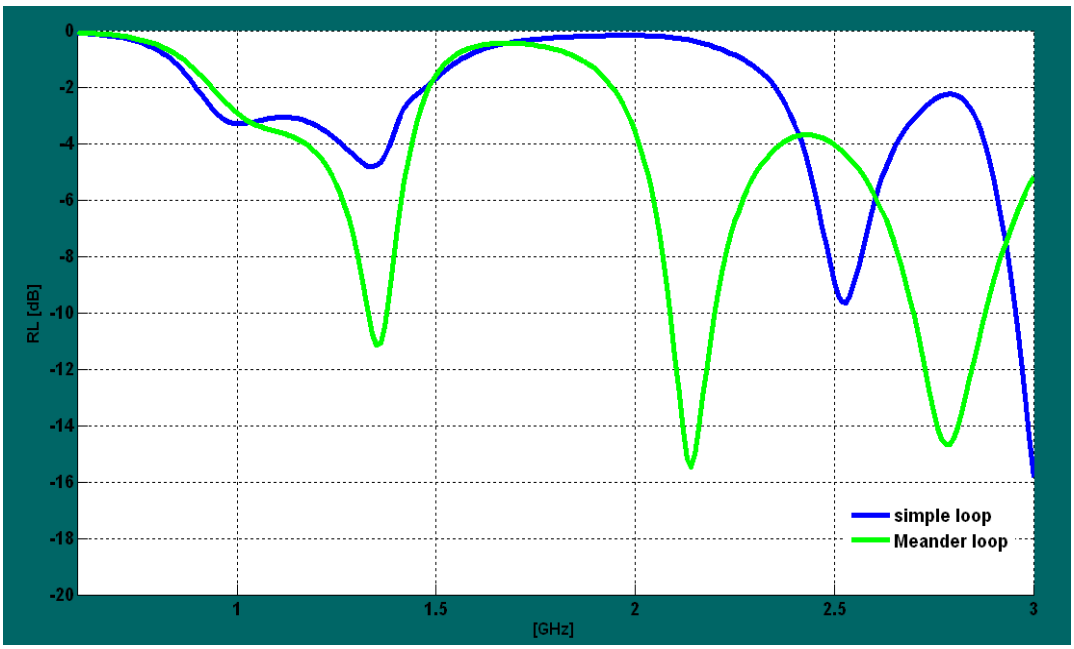

Fig.3.4. Comparison of S11 for simple and meander loop.

The effect of increase in the width of the carrier, height of an antenna from the ground plane and ground length has been seen in Fig.3.5. It improves the lower bandwidth and helps to cover the lower bands as it has bandwidth potential. As the work is limited to a fixed geometry, section 3.5 focuses on the proposed design.

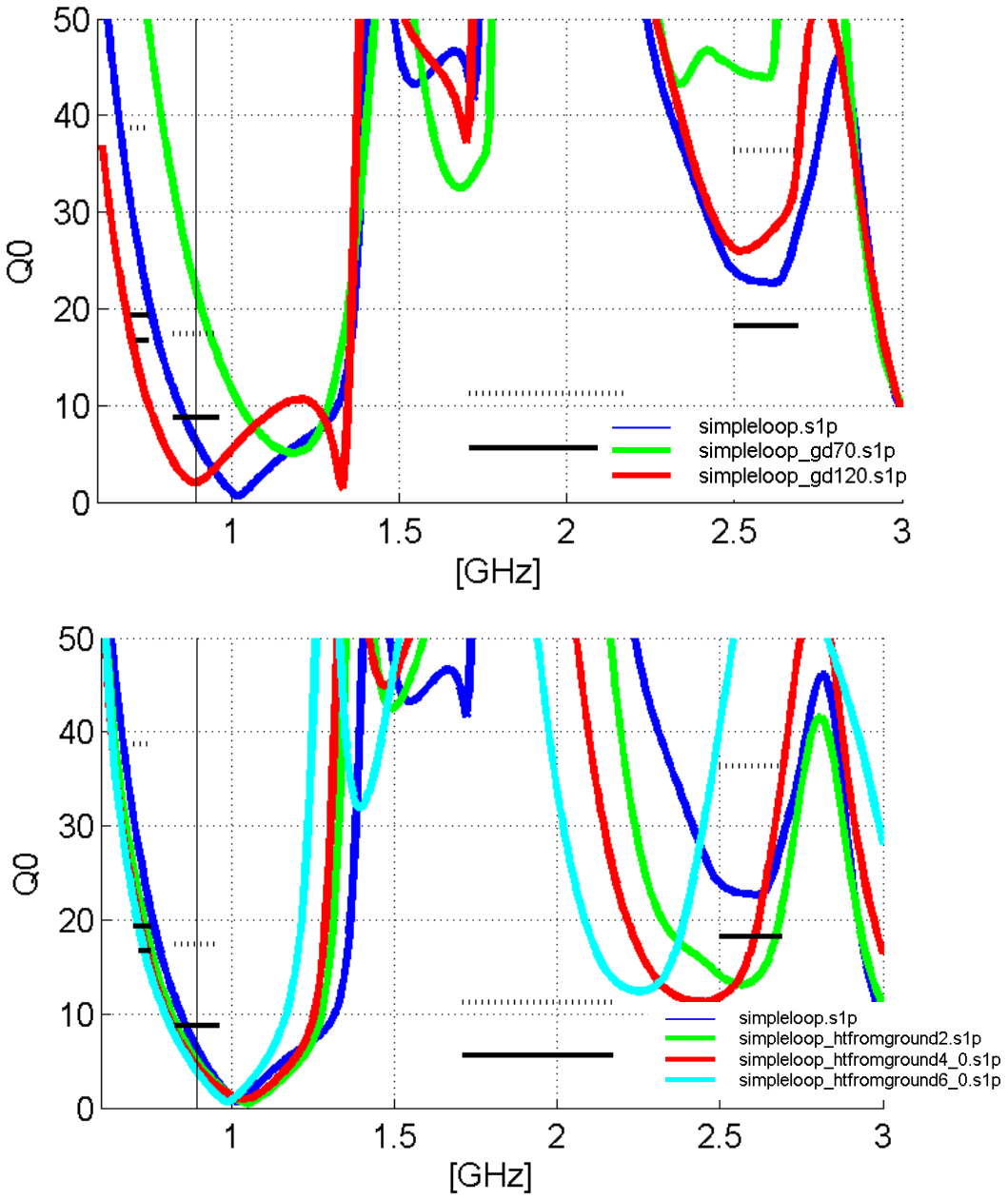

Fig.3.5. Influence on Q factor by changing the (a) ground length and (b) height of the antenna.

3.5 Proposed design

So far, simulations have shown that the loop has the potential for multiband coverage. In order to decrease the fundamental resonance frequency and to properly excite the modes for 900MHz, 1800MHz and 2600MHz, meandering is incorporated in the loop structure.

Consider the meander line antenna where several lines are placed parallel to each other. The surface currents along the horizontal and vertical lines depend on the number of turns, spacing between the lines and the width of lines. It makes the antenna to resonate at the right frequencies and achieve the required bandwidths as given in Table.3.1.

The impedance matching of such a small antennas in a wide frequency range is somehow difficult. It is possible to increase the bandwidth by using multiple strips because the radiation resistance can be stepped up and the reactances can be made to cancel each other in the balanced and unbalanced current modes. More turns of meander line traces can reduce the operating frequency of the fundamental mode [19]. A HFSS design model is shown in the Fig.3.6. It comprises a carrier, ground plane and radiating antenna element. A lumped port of 50Ω is used to launch the signal at one end while the other end is connected to ground.

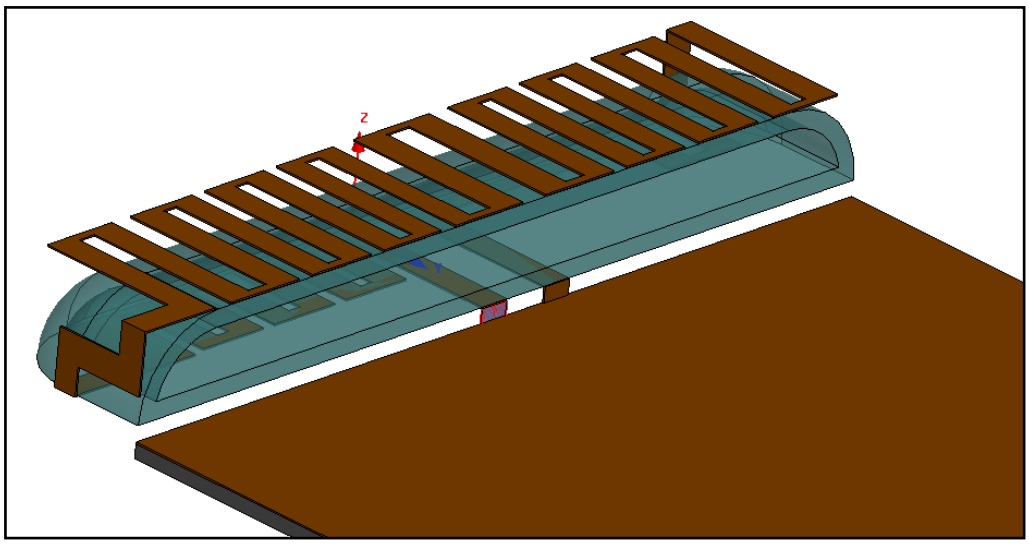

Fig.3.6. Simulated proposed design in HFSS.

The mutual capacitance between the lines strictly depends on the distance between them. Increasing the distance between two copper strips or decreasing the strip width in the meanderline reduces the mutual coupling and the resonance frequency shifts down adding inductance to the resonant system [20]. A thinner substrate of 1mm thickness would also enhance the resonant coupling between the lines. The reduced near field strengths in meander line antenna is because of the spatially distributed radiating elements. The copper strip placement takes the round edges of the carrier structure into consideration.

3.6 Simulation results

The antenna structure is tuned to get optimum bandwidth at all the frequency bands with return loss better than 6dB and acceptable radiation performance. Fig.3.7.and Fig.3.8, shows the return loss optimization by changing the line spacing and gap of lower part of radiator from the ground plane respectively.

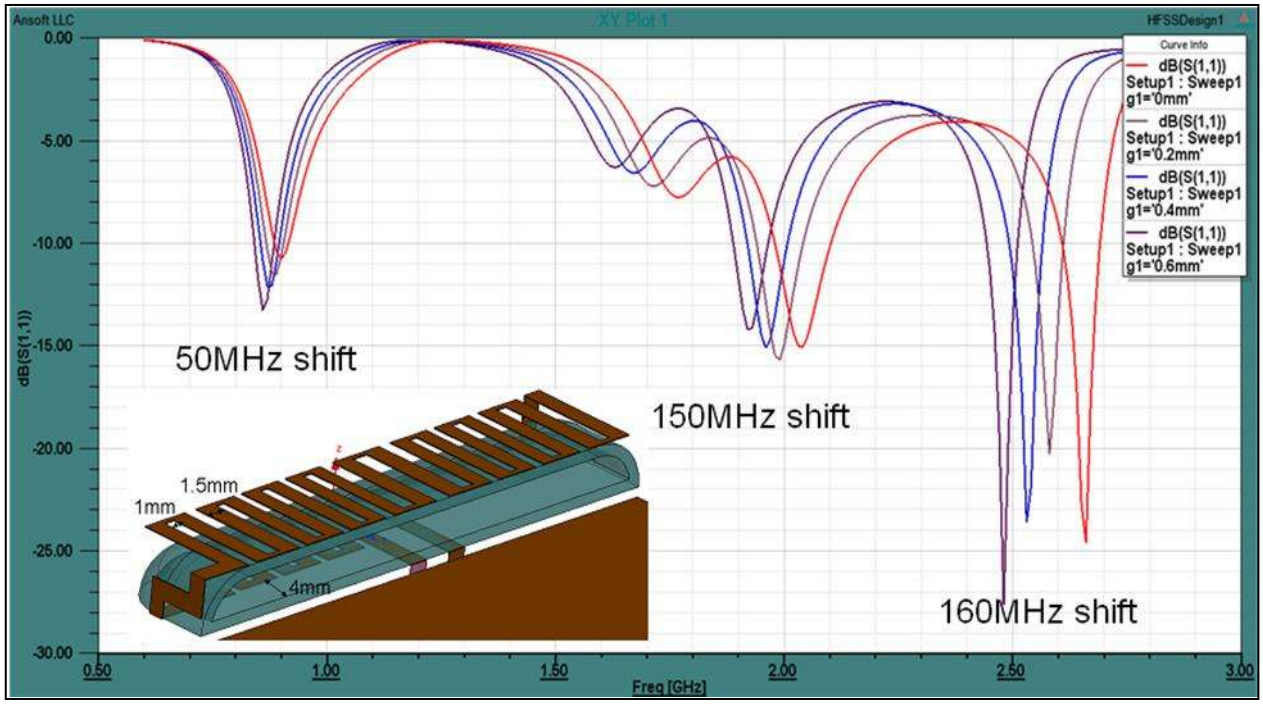

Fig.3.7. Optimization of the line spacing.

Fig.3.7 shows that by decreasing the line spacing from 1.6mm (Violet) to 1mm (Red Curve) there is a dominant shift in the higher band frequency. Thus the mutual coupling between the lines is stronger for higher frequencies. Similarly Fig.3.8 shows,

increasing the gap between the lower radiator and the ground plane improves the high band response. The red curve is for 4mm gap and the violet curve is for full length of the lower radiator, i.e there is no gap from the ground plane.

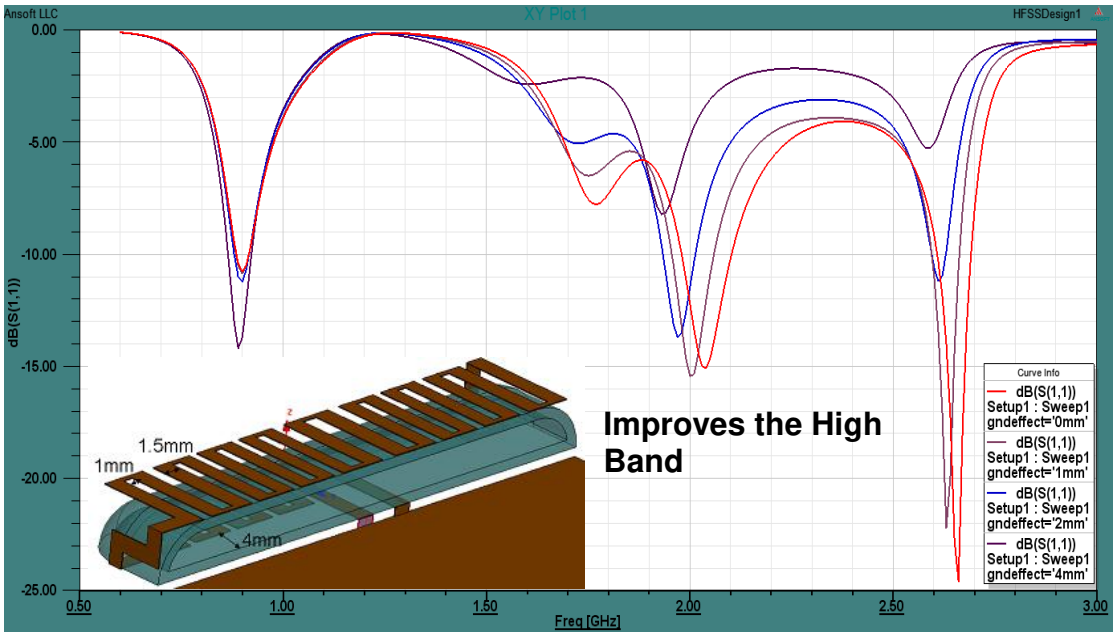

Fig.3.8. Optimization of the gap from the ground plane.

The finally optimized results are shown in Fig.3.9.As the frequency increases, the operating modes have not only wider bandwidth but also better return loss values. The antenna is exhibiting the desired matching without the use of parasitic radiator.

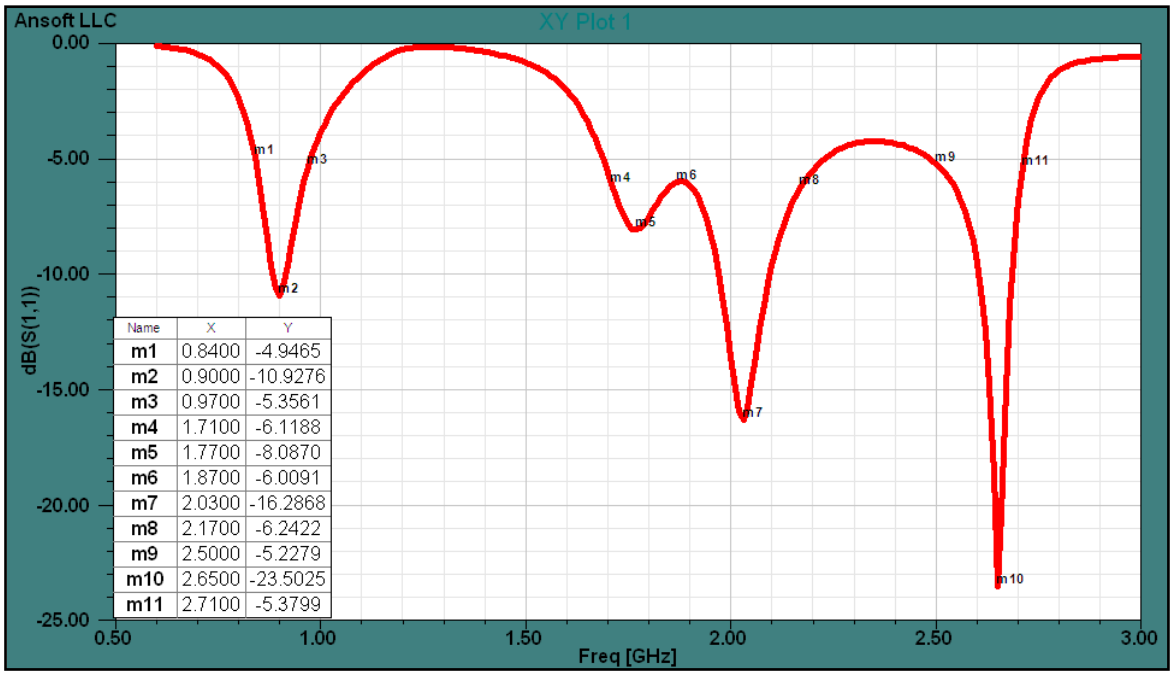

Name	X	Y
m1	0.8400	-4.9465
m2	0.9000	-10.9276
m3	0.9700	-5.3561
m4	1.7100	-6.1188
m5	1.7700	-8.0870
m6	1.8700	-6.0091
m7	2.0300	-16.2868
m8	2.1700	-6.2422
m9	2.5000	-5.2279
m10	2.6500	-23.5025
m11	2.7100	-5.3799

Fig.3.9. Simulated S11 of proposed design.

From the impedance plots Fig.3.10 and Fig.3.11, multiple resonances occur at 0.9, 1.77, 2.03 and 2.65 GHz. The real part is good enough to be matched to 50Ω port impedance. From the plot two more resonances at 1.1 and 2.5GHz occur but the real part is too high which can not be matched to the port impedance.

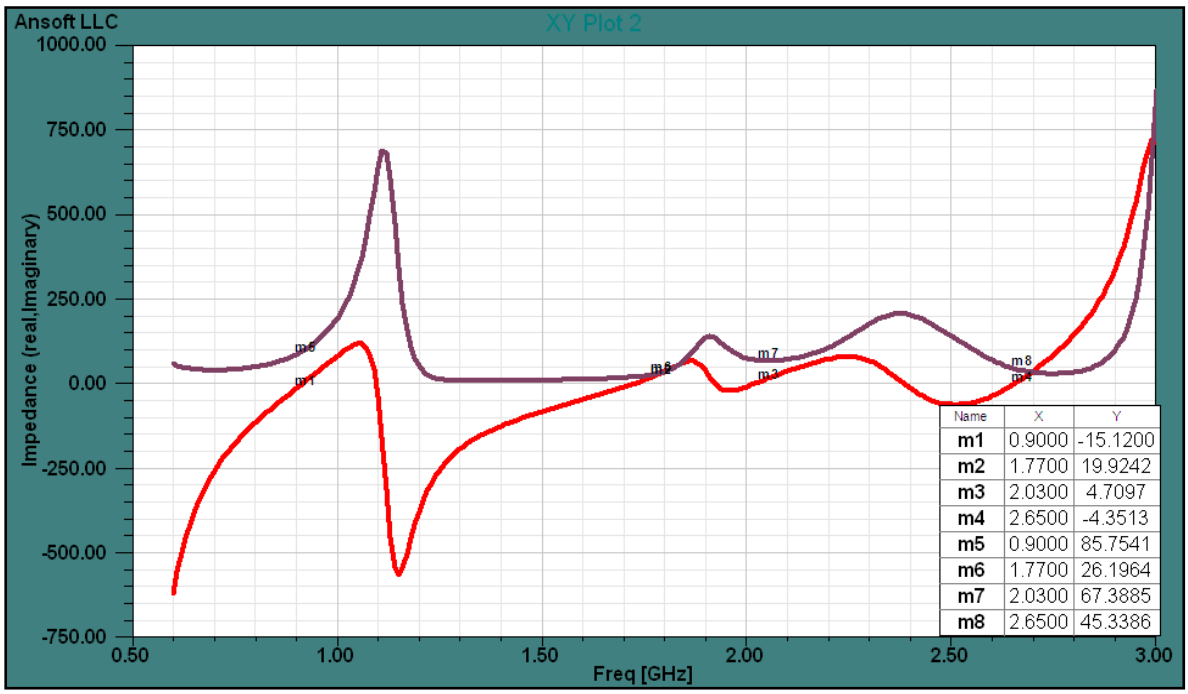

Fig.3.10. Simulated impedance plot of proposed design.

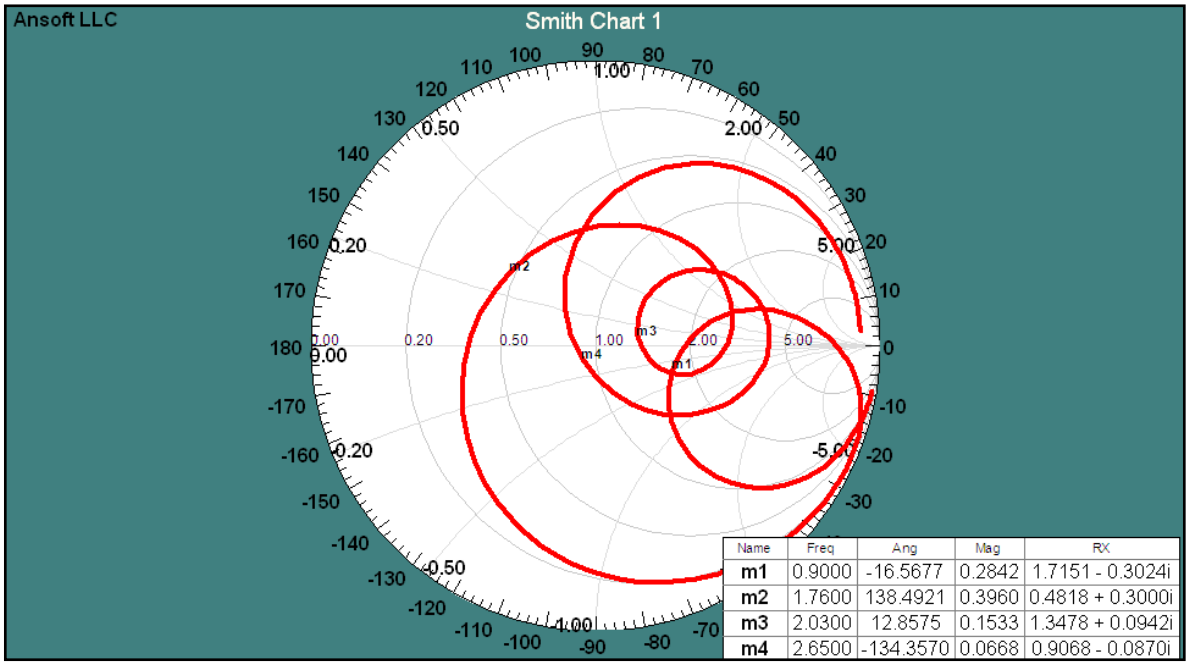

Fig.3.11 Smith plot of proposed design.

3.6.1 Surface Current Plots

The current distribution plots are taken from the simulations as shown in Fig.3.12 (a, b, c, d &e). For first resonance λ/2 or 0.9GHz one null occurs at the center and for 3λ/2 mode three nulls occur for the frequency of 2.03 GHz and 2.65GHz. The current directions are opposite making an unbalanced mode, see Fig 3.12 (a, d &e).

For the balanced mode, which is the λ mode, two nulls occur and the current is in the same direction making a closed loop on the antenna element and creating opposite currents on the chassis as can be seen from Fig.3.12 (b &c) .The frequency from 1.76GHz to 1.98GHz exhibits the balanced mode. The current null on the chassis can also be seen from these plots.

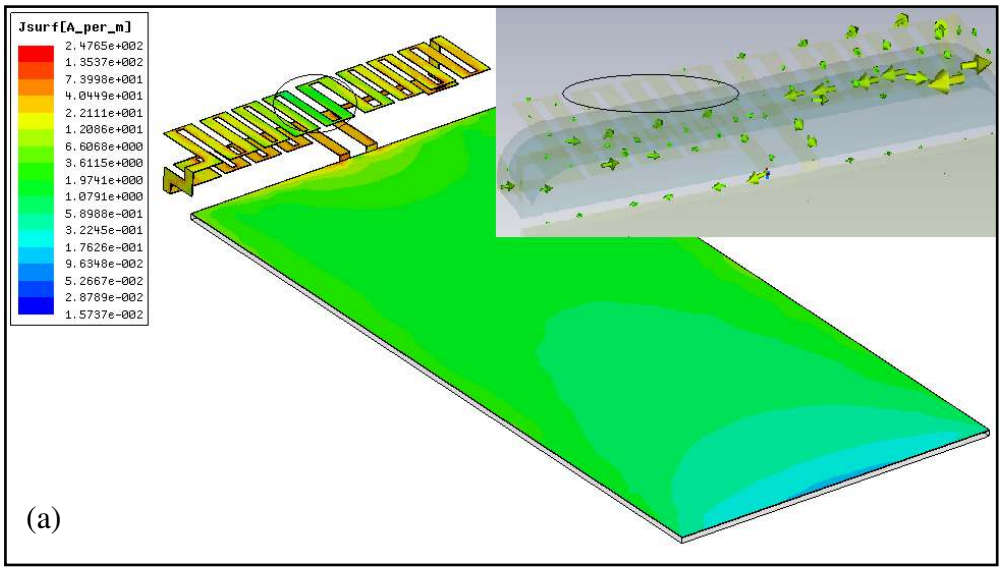

(a)

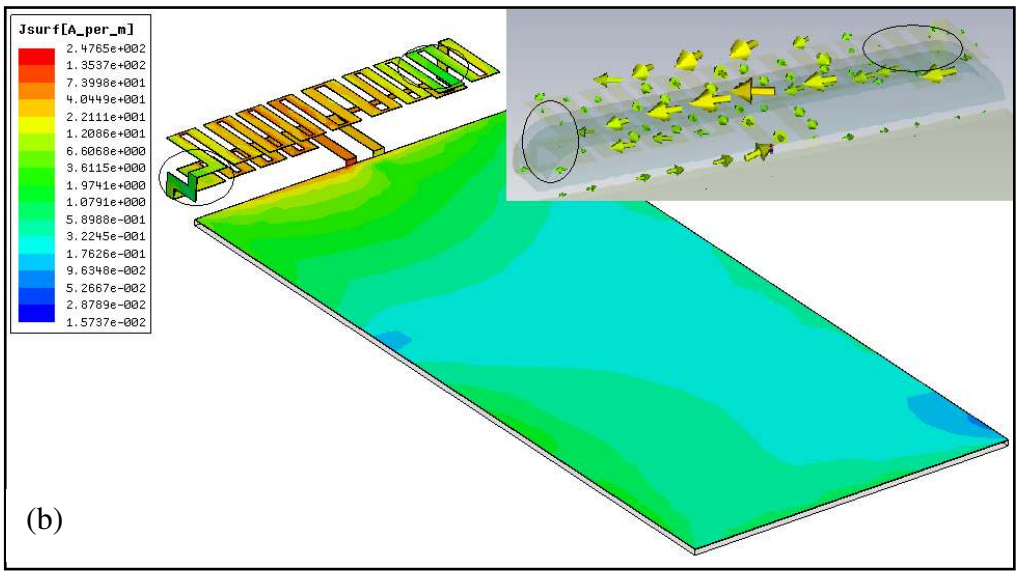

(b)

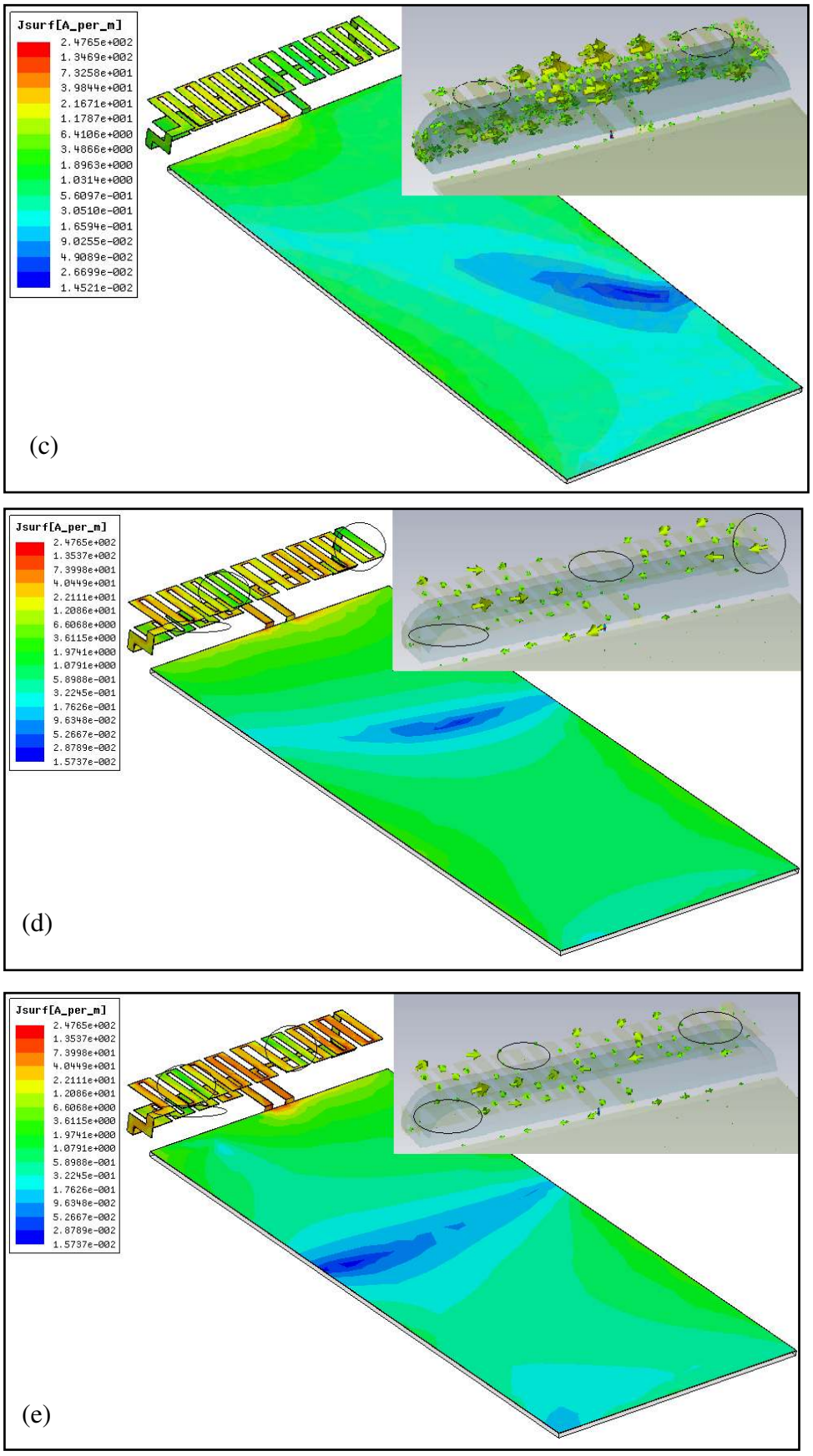

Fig.3.12. Surface current density plots for (a) 0.9GHz (b) 1.76GHz (c) 1.98GHz (d) 2.03GHz and (e) 2.65GHz.

3.7 Fabrication

The design is printed on Kapton flexfilm. The antenna carrier is a 3D-object with rounded corners requiring an accurate and careful placement of the 2D-flexfilm. Excitation is applied through the cable. A prototype is shown in Fig. 3.13.

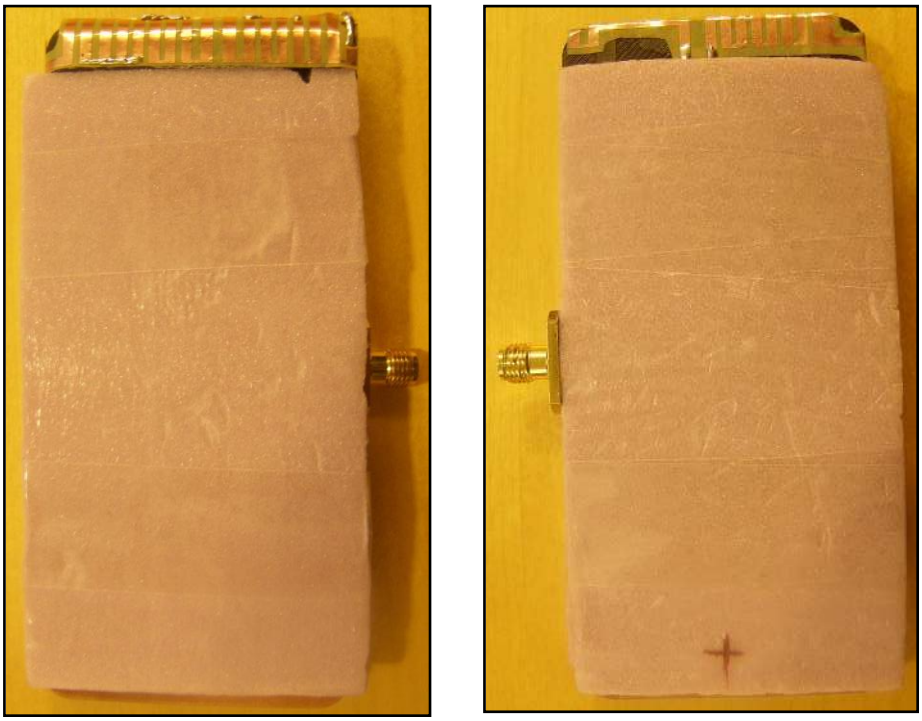

Fig.3.13. Fabricated prototype front and back view.

3.8 Measured results

Return loss and efficiency measurements are done using a network analyzer, and an anechoic chamber, respectively. The measured results are in good agreement with the simulated results. Fig.3.14. shows the measured return loss for the prototype. In the simulation the effect of the flexfilm has not been considered that is why in the fabricated prototype, a shift in the frequency has been observed. Tuning is done to move the frequency at the required resonant points that can be seen from Fig.3.13. A reduction in 6dB BW has also been observed in higher band of 2.6GHz.

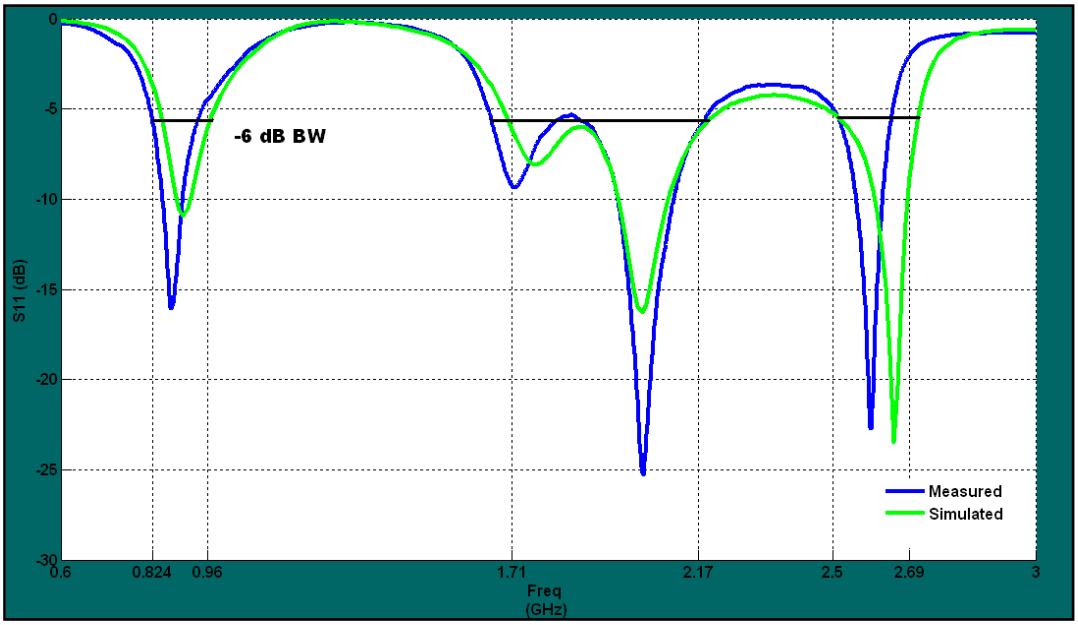

Fig.3.14. Comparison of simulated and measured S11.

Overall radiation η is good .For the lower band (900MHz), first higher (2000MHz) and second higher band (2600MHz) it is better than -1dB,-1.8dB and -2.5dB respectively, c.f Fig.3.15.The overall total η is less than -3dB, but for frequency greater than 2.63GHz it goes worse as the S11 is not good in the measured prototype.

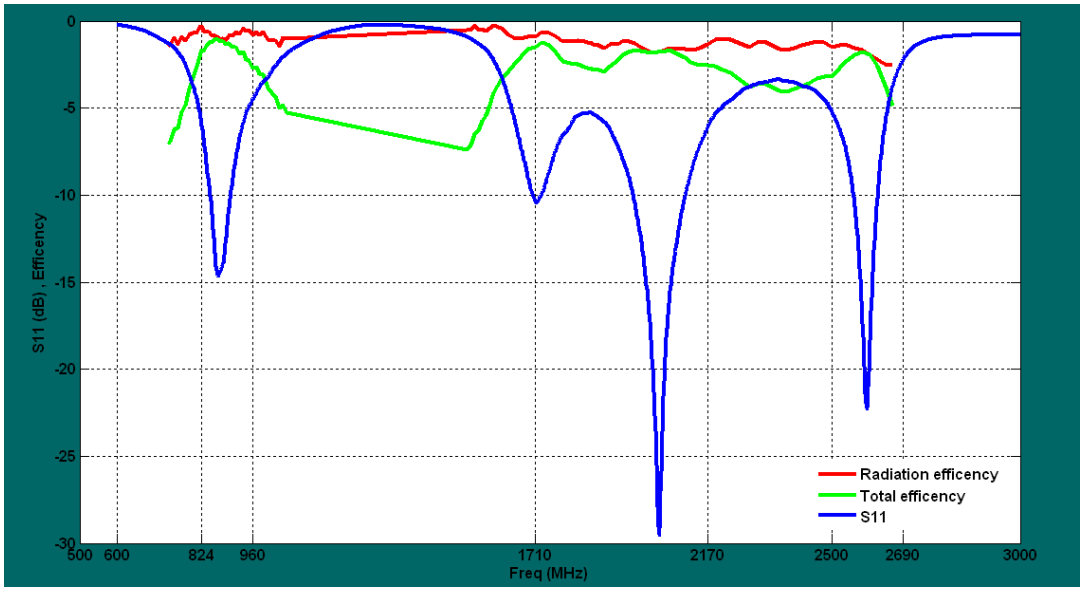

Fig.3.15. Measured S11, total η and radiation η.

3.9 Head and hand effects

The effect of head and hand is also seen. η measurements are done in Satimo anechoic chambers. Fig.3.16 (a) shows the placement of handset near the right side of the head and (b) shows the handset in hand beside head. The placement of handset has to be accurate to make it as close to real life scenario as possible.

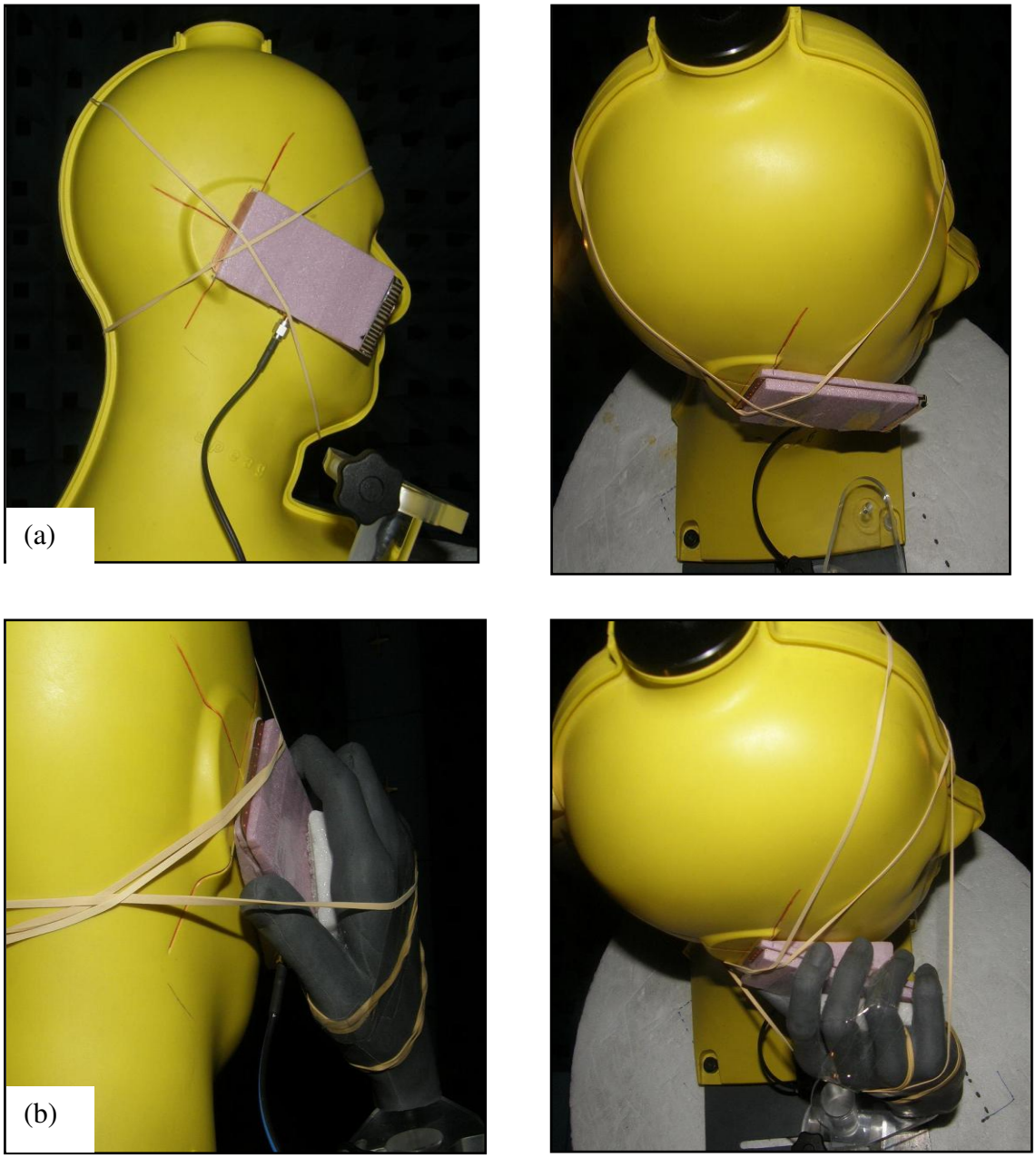

Fig.3.16. Measurement setup for efficiency measurements of antenna (a) besides right side of head and (b) besides head with hand.

Total η reduces by 2 to 3 dB while very less detuning has been observed in the presence of head for all the bands. High detuning has been seen when the handset is placed inside hand and near the head the lower band and second higher band i.e. 0.9GHz and 2.6GHz respectively, see Fig.3.17. While very little effect has been seen for the balanced mode 1.8GHz to 2GHz. From Fig.3.18 approximately 4.5 dB and 10dB radiation efficiency loss has been measured with head only, and head & hand respectively for the lower band and approximately 2.5 and 6dB radiation efficiency loss by head only and head & hand respectively for higher band.

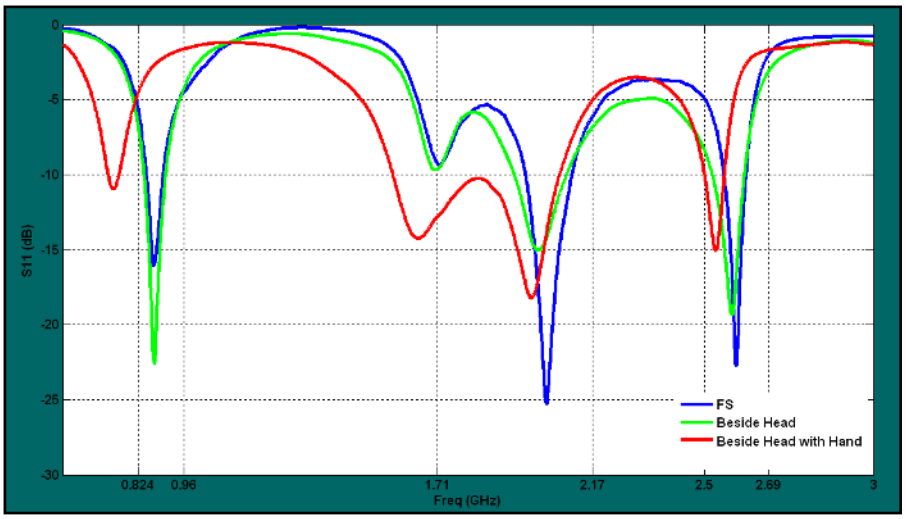

Fig.3.17. Comparison of S11 for free space, beside head and beside head with hand.

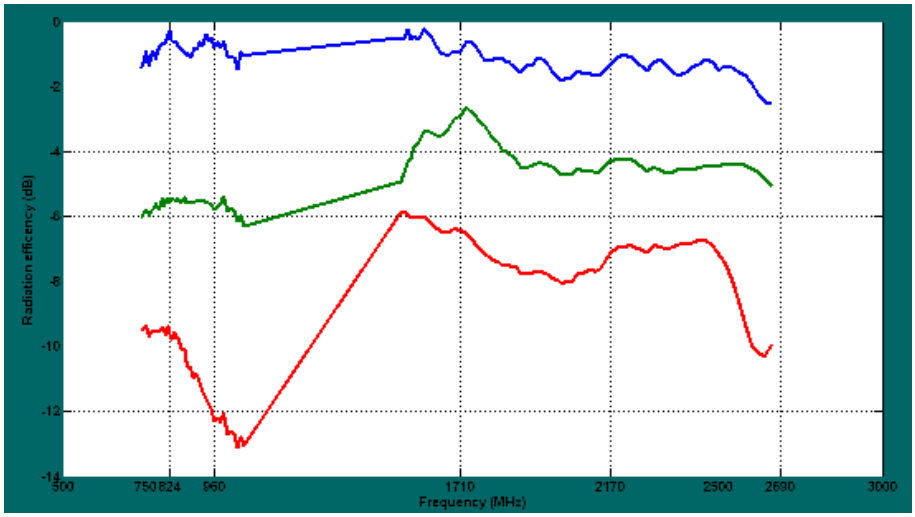

Fig.3.18. Comparison of radiation efficiency for free space, beside head and beside head with hand.

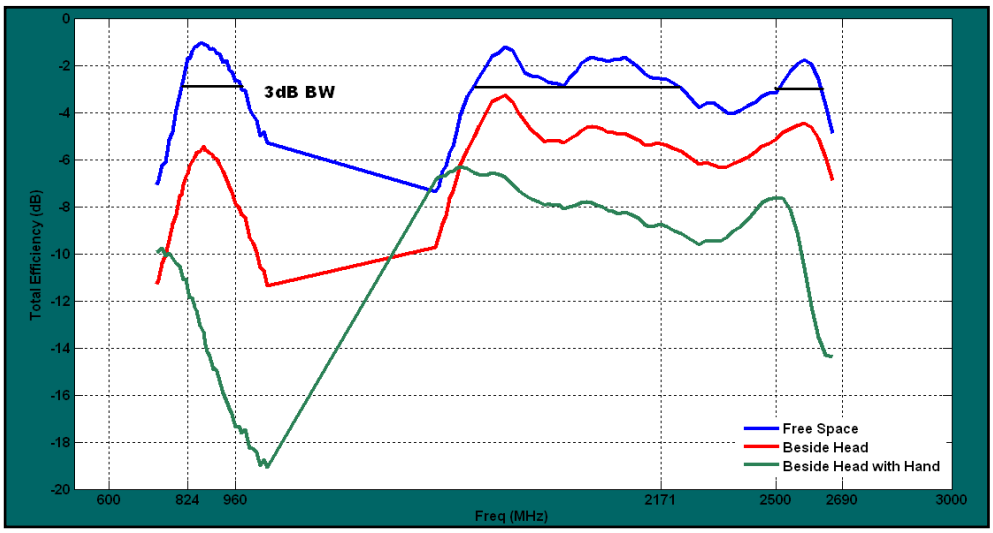

Fig.3.19. Comparison of total η for free space, beside head and beside head with hand.

The fabricated prototype has shown consistent results with the simulated results. This antenna has the ability to operate at multiple frequency bands simultaneously without dynamic detuning, is highly efficient in terms of small volumetric size for a given bandwidth of operation.

CHAPTER: 4 SPECIFIC ABSORPTION RATE (SAR)

4.1 Introduction

In order to communicate to the network, mobile phones transmit signals of certain power. In the last few years there have been implementations of standards regarding the human health safety, which puts some restrictions on the amount of power going towards the user.

All the electronic devices emit radiations to some extent, while in antennas it is planned to transmit or receive the electromagnetic waves to establish a communication link, which makes it an essential part of all communication devices.

Communication devices use some kind of antennas, which are radiating energy isotropically or directionally. The fields emerging from the antennas are mainly classified as near fields and far fields. In the near field region, the fields are more reactive and have more losses. To some extend it is possible to control the level of power absorption into the user with a good antenna design. One approach is to design an antenna which has minimum near field emissions in particular direction. Another approach is to place the antenna at the bottom of the device, so more radiations would be away from the head. Mobile phones antennas are designed to operate within these stringent limits in order to compliance with the standards of exposure to these radiations, named as SAR.

SAR describes the absorption of power into lossy medium (human body) as a result of the electric fields and currents present in the tissue.
Mathematically,

$$SAR = \frac{\sigma \cdot (|E|)^2}{\rho}$$

Where σ is the conductivity (S/m), E is the induced electric field intensity, (V/m) and ρ is the mass density of tissues (kg/m^3).

SAR has units of watts per kilogram or milliwatts per gram. It has different limits for different regions of the body, as well as the volume over which the average is made. SAR values for 1g or 10g averaging volume are more commonly considered.

US and Europe have different standardized values. Spatial peak SAR, head and trunk (W/kg) should not exceed 1.6 as averaged over 1g for US, and 2 as averaged over 10g for Europe [21].

To ensure the public safety, all radio communication devices need to fulfill the FCC or ICNIRP or IEEE safety regulations before coming to the market [22]. A standard procedure for testing these devices has been governed with defined limitations on absorption of energy into body tissues.

4.2 Body Effects

One can assume human body as a relatively good conductor compared to the surrounding air medium and it can act as a receiving antenna. Human body is comprised of tissues, which are made up of water, salts and different organic compounds. Muscles and organs contain more water and are good conductors as compared to fats or bones. The effects caused by these strong fields can be heating of tissues and stimulation of the nerves [22].

The fields are coupled to the body and affect the tissue, cells, bones and liquid of the body. The absorption rate is not only a function of the field strengths and frequency but also the shape and size of the user and location of the device has shown influence.

While using a mobile phone there is a constant electromagnetic coupling to the body, which increases the body temperature. These disruptions can cause temporary or permanent destruction of body cells, depending on the level of exposure.

The influence of the user body especially head and hand, to the reactive near fields of the antenna and the chassis can change the radiation efficiency, SAR and the center frequency of the antenna.

4.3 Simulation Setup

As explained earlier, an important issue regarding the usage of handset is the absorption of electromagnetic radiation to the exposed user. After 1996, all the handsets are required to meet the SAR standards, so it has become an important parameter before launching the new model. An estimate of the SAR for the proposed design has been done in the CST simulations at different frequencies.

In all the advanced EDA software, a provision to calculate the SAR has been provided. A phantom model having exact shape and size as according to the IEEE/ANSI C95.1 standards has been used. The material properties for the homogeneous fluid that emulates the characteristics of tissue and a head shell specifying the conductivity are defined. There are two typical positions of placing the device, cheek and tilted. It is obvious to have high SAR value at cheek position as compared to the tilted one, as device would be farther away. The exact gap definition between the device and user head is very important to get the accurate results.

As shown in the above equation, SAR is calculated from the total electric field strength, the conductivity of the medium and the density of the mass. In the simulations the power loss density monitor is defined. The electric conductivity (0.0016 S/m) for the head shell, liquid density (1000 kg/m^3) and 2nd order dispersive model for epsilon is specified to the head model for the frequencies of interest.

A phantom head with the prototype is simulated in a typical right hand side scenario and shown in Fig.4.1.

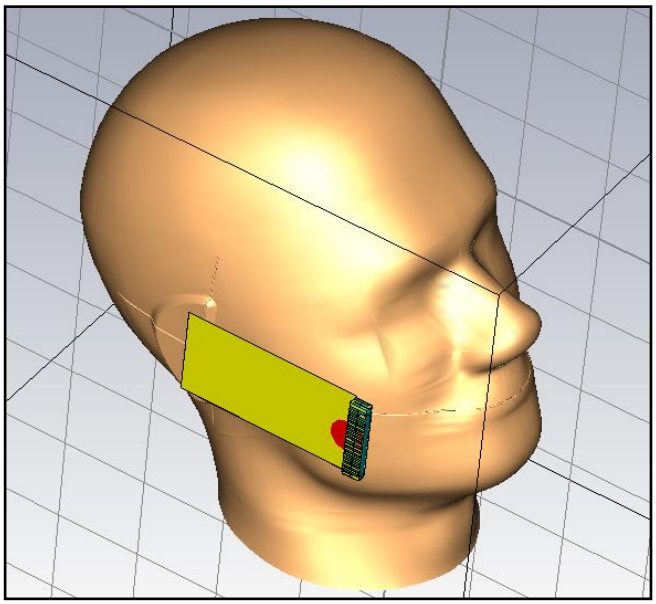

Fig.4.1.Placement of prototype with Phantom head model in CST MWS.

The simulated results for 894MHz, 1710MHz, 1895MHz, 1980MHz and 2560MHz for 1g (right side) and 10g (left side) averaging are shown in Fig. 4.2.

It can be seen from the Fig.4.2 that at different frequencies the location of maxima on the chassis changes. As the chassis length at GSM 900 is less than half of a wavelength only one field maxima at the center occurs, while for 1710MHz it indicates a shift of the maxima towards the antenna. For 1980MHz chassis is near to have two resonating modes and for 2560MHz it completely resonates for two modes.

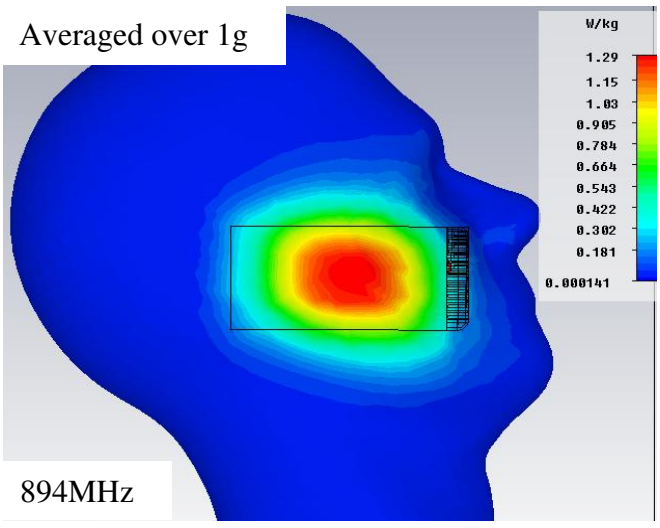

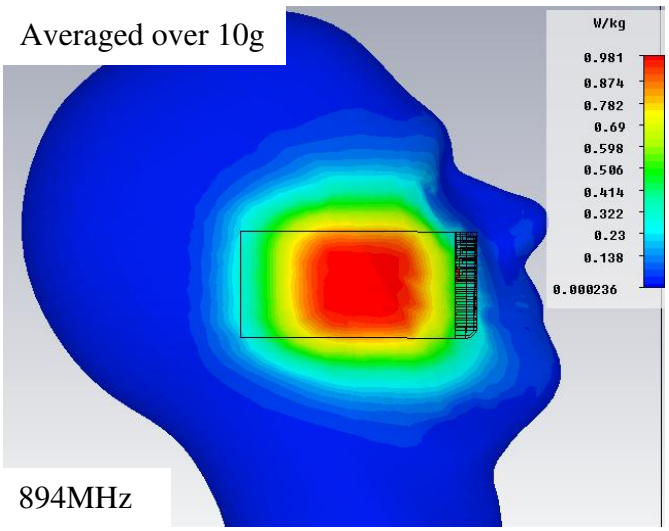

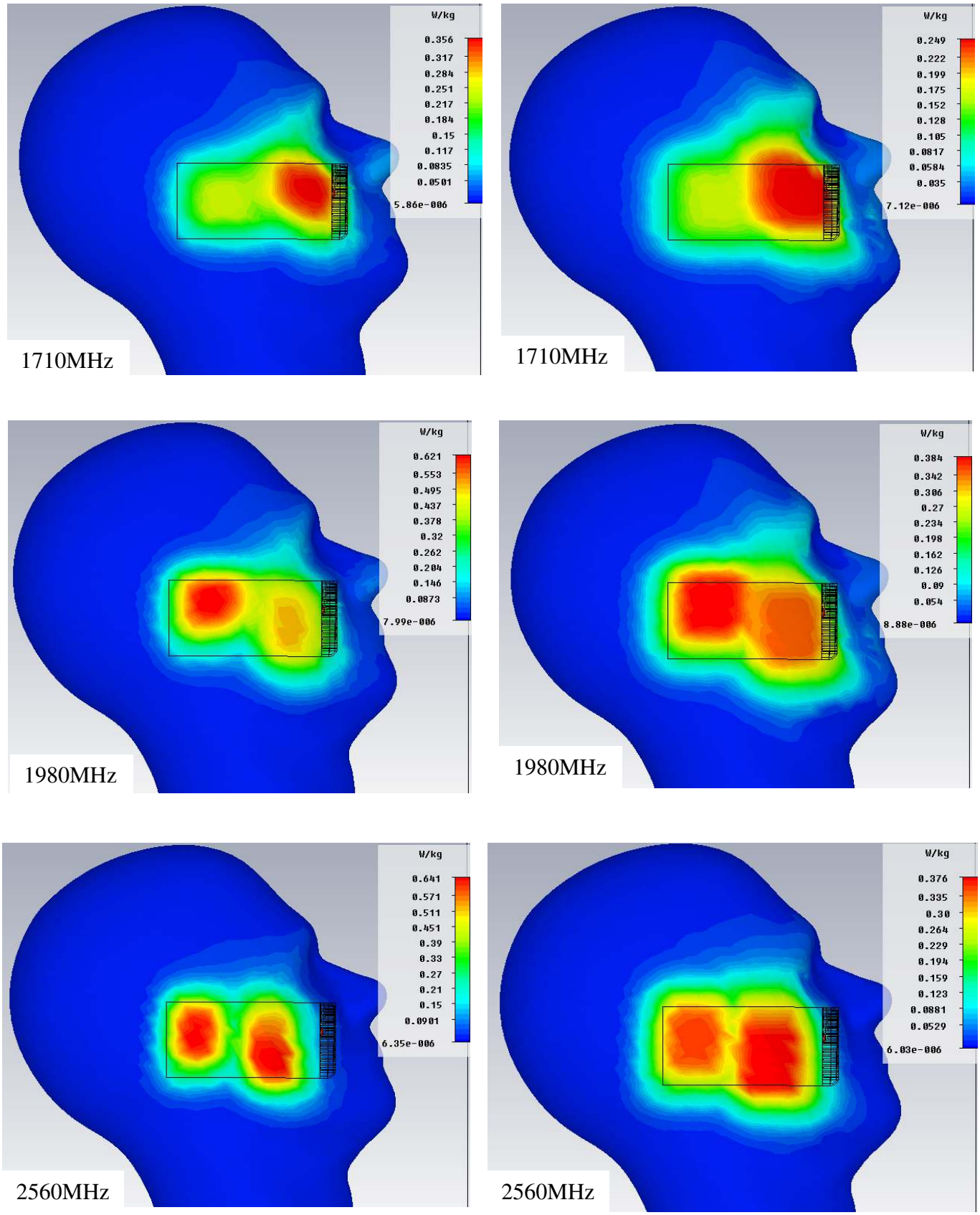

Fig.4.2. Simulated SAR for 1g and 10g averaging at 894, 1710, 1895, 1980MHz and 2560MHz.

For 900MHz which is unbalanced mode, the maximum value of SAR has occurred that indicates the size of the antenna is small and the currents are going towards the chassis. These currents on chassis can cause high absorption rate to the user and can decrease the efficiency.

An obvious relationship between bandwidth, efficiency and SAR can be established here. In order to cover lower band whole metallic chassis contributes with the antenna but at the same time reduces the efficiency and increases the SAR.

A quick check has been done on the efficiency of the antenna when placed near the phantom head. The simulated radiation efficiency values at different frequency are as below in the Table 4.1.

Frequency (MHz)	**Radiation Efficiency without phantom head (dB)**	**Radiation Efficiency with phantom head (dB)**
894	-0.99	-4.61
1710	-0.98	-1.93
1895	-0.97	-1.74
1980	-0.97	-2.17
2560	-0.91	-2.69

Table.4.1 Simulated radiation efficiency for the antenna placed near to Phantom head.

Hence the decrease in the radiation efficiency at lower frequency has predominant effect as compared to the balanced mode frequency of 1710 and 1895 MHz [23, 24].

4.4 Measurement Setup

SAR measurements are time taking and requires a lot of accuracy in terms of the placement of the device along with the phantom head, simulated liquid material properties, and probe calibration and positing to measure the field strength.

Measurements are done on DASY4 equipment which consists of a dipole for pre system accuracy check, a device holder, phantom head and body model with tissue simulating liquid, a robot, a probe with optical surface detection, data acquisition unit and DAYS software as shown in Fig.4.3(a) and (b).

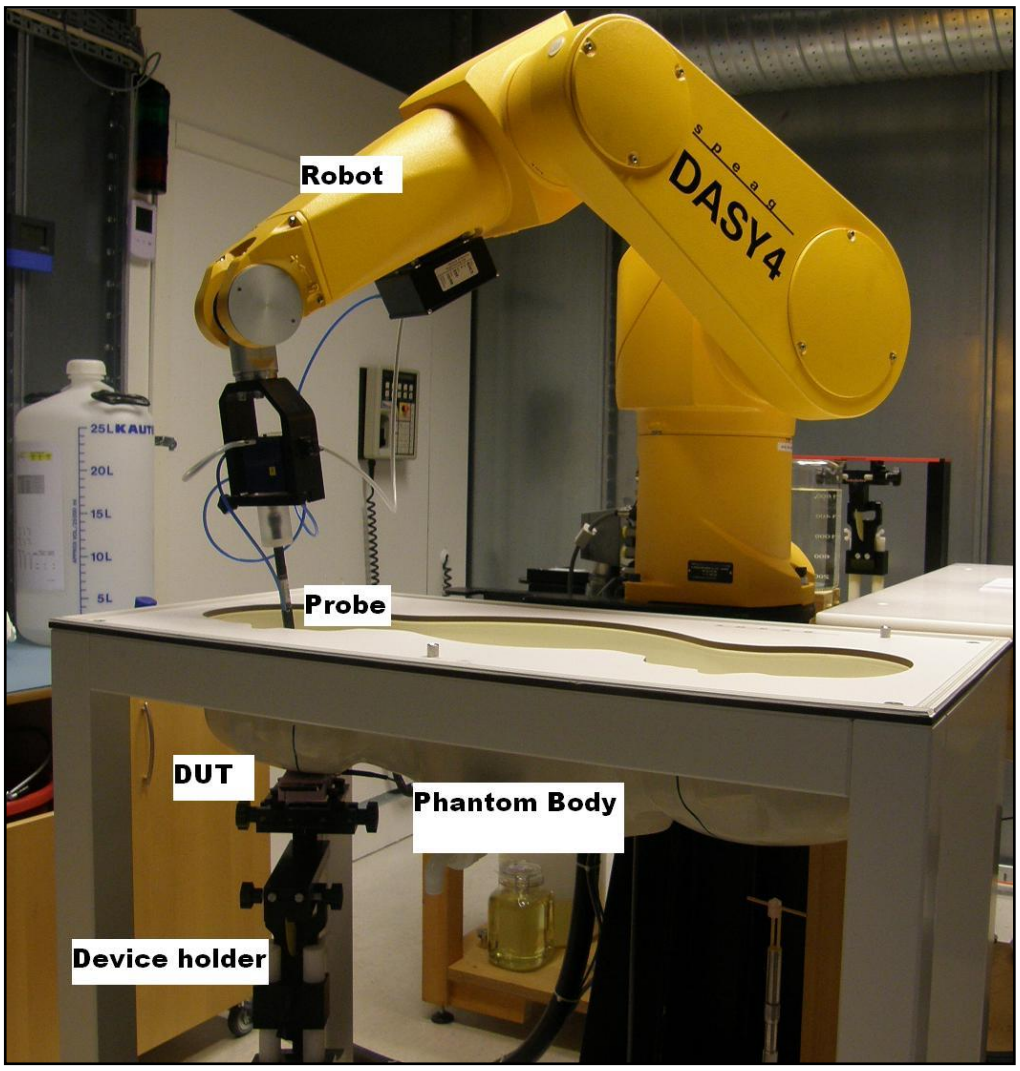

Fig.4.3.a. Measurement setup for DASY4 equipment.

The measurements are started by doing system calibrations, then placing the DUT accurately and firmly near the cheek. Proper alignment is very much important. Probe scans the whole area and marks the peak SAR position that can be seen on the software. Then makes the volume for 1g cube or 10g cube to calculate the averaged SAR value.

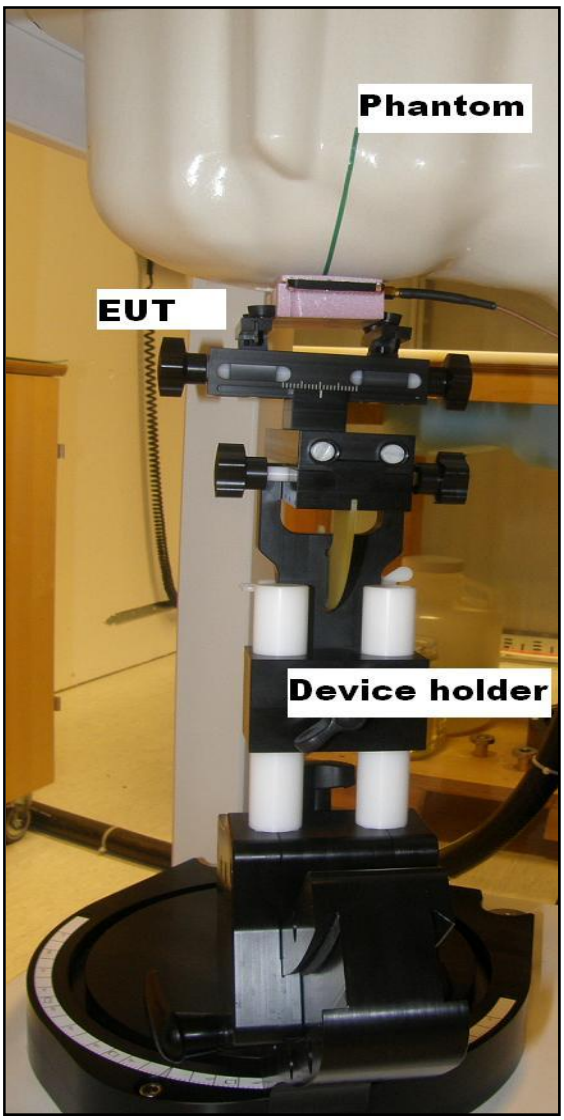

Fig.4.3.b. Close view of the equipment under test (EUT) with the Phantom head.

4.4.1 Measured results

Fig.4.4 shows the measured results for the SAR, giving the peak SAR location and field maxima on the chassis for the associated frequency.

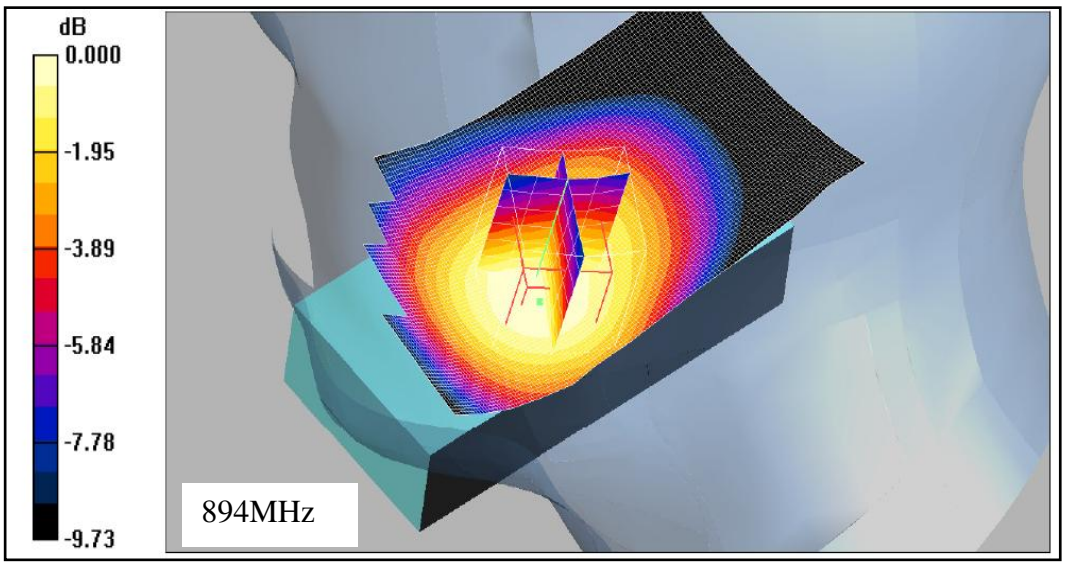

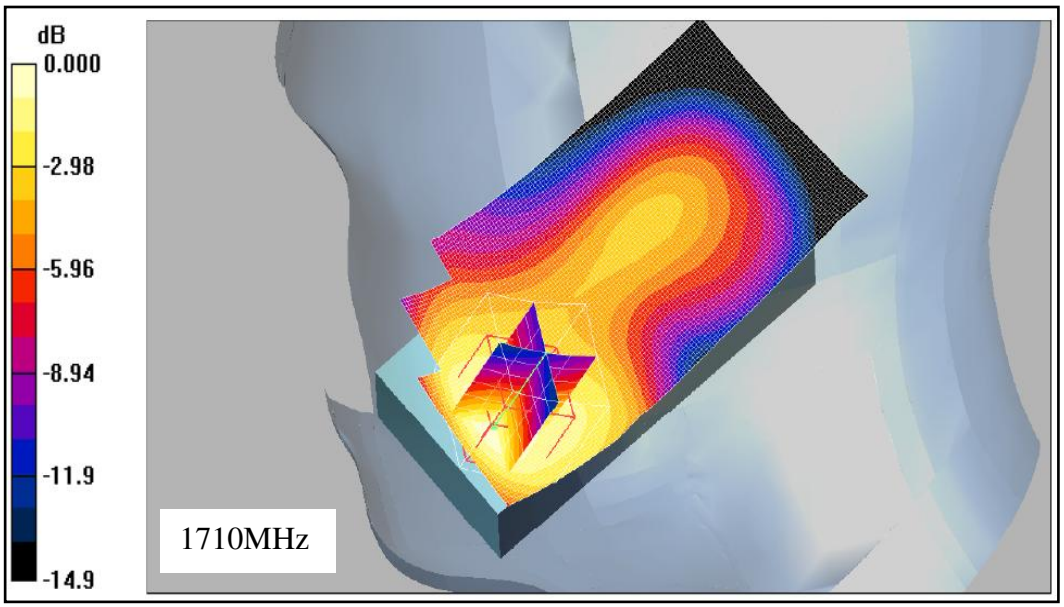

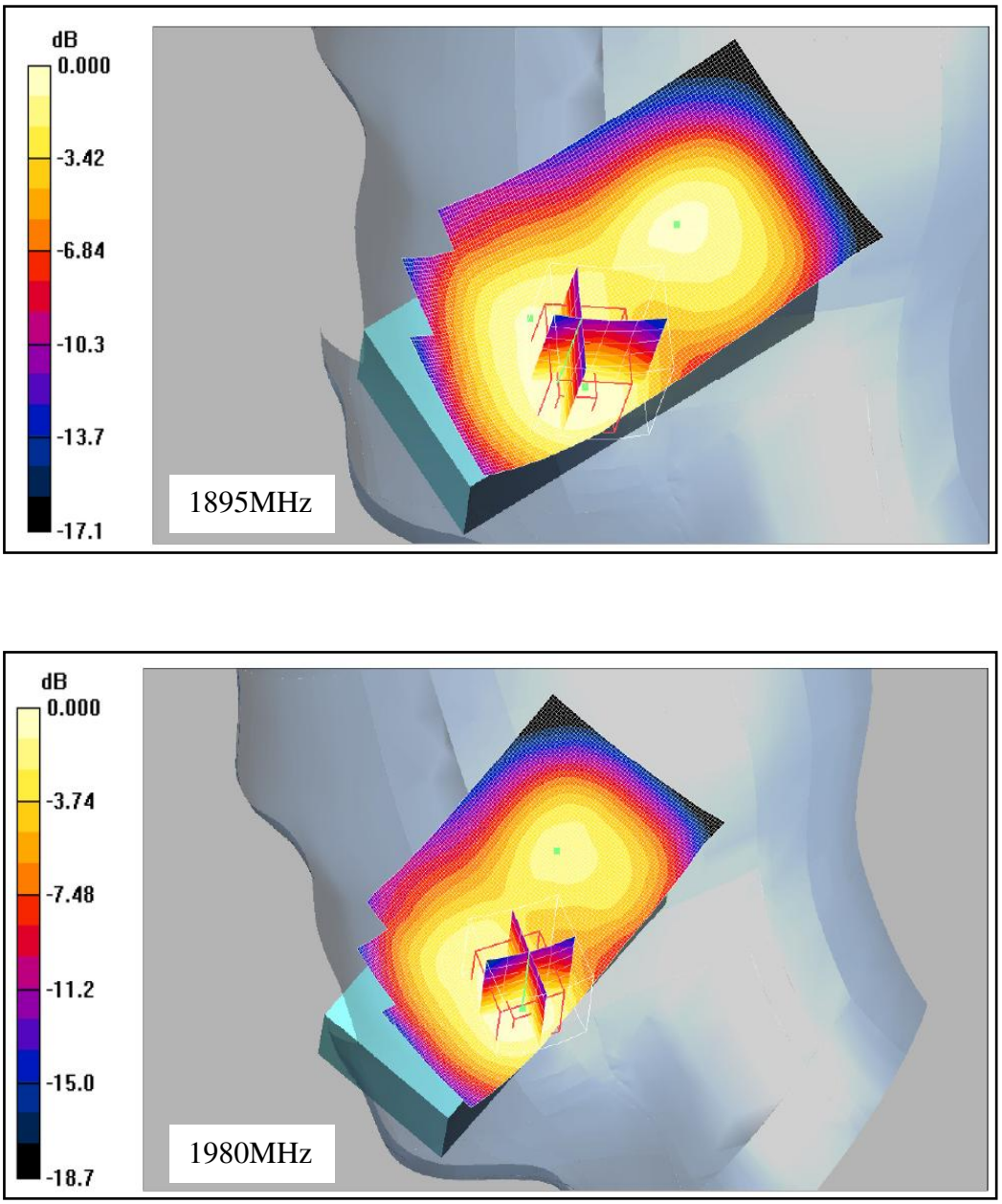

Fig.4.4. Measured results at 894MHz, 1710MHz, 1895MHz and 1980MHz for the prototype.

It has been already explained in the simulation results about the response of resonating modes of chassis. The green spot are the hot spots and two cubes can be seen, one for the 1g and other bigger one is for 10g averaging mass. The measured and simulated SAR results are compared in the Table.4.2.In measurements 2560MHz has not been covered because of some limitations of hardware.

Frequency (MHz)	SAR Simulated (mW/g)		SAR Measured (mW/g)	
	1g	10 g	1g	10 g
894	1.29	0.98	1.72	1.26
1710	0.36	0.23	0.48	0.29
1895	0.47	0.32	0.93	0.59
1980	0.62	0.38	0.93	0.57
2560	0.64	0.38	-	-

Table.4.2. Comparison of the measured and simulated SAR values.

SAR values at 900MHz is almost double than that at 1895GHz, which is a expected result, complying the radiation efficiency to reduce in the same fashion. One can see certain agreement between the simulated and measured results. The possible reasons of deviation of the results can be the difference in the human body emulated liquid properties used in the measurements and assigned in the simulation setup. The SAR averaging method used in software simulations is IEEE C95.3, while in measurements IEEE Standard 1528-2003 has been employed.

Chapter: 5 Hearing Aid Compatibility (HAC)

5.1 Introduction

With the recent advancements in mobile phone and hand held devices there is emphasis not only on reducing the size of the antenna and improving the power efficiency but also on meeting the new FCC standards for SAR and HAC, which mainly depends on the near field emissions [25].

All portable devices are required to meet the HAC standard ANSI C63.19 that was approved in 2001 and according to the standard, half of all the mobile phones in the U.S.A market must have RF interference level of at least M3 or M4 category in all frequency bands [26]. The idea behind this requirement is to relax the ear piece area from RF emissions. For this the hearing aids are rated for interference rejection and mobile phones are rated for the generated RF emission. In the ANSI standard, a set of values have been given for E and H near field strengths for the frequency greater than or less than 960MHz c.f Table 5.1 [25].

Category	AWF (dB)	Limits for E-Field Emissions (V/m) > 960MHz	Limits for H-Field Emissions (A/m) > 960MHz
M1	0	199.5 - 354.8	0.6 - 1.07
	-5	149.6 - 266.1	0.45 - 0.8
M2	0	112.2 - 199.5	0.34 - 0.6
	-5	84.1 - 149.6	0.25 - 0.45
M3	0	63.1 - 112.2	0.19 - 0.34
	-5	47.3 - 84.1	0.14 - 0.25
M4	0	<63.1	<0.19
	-5	<47.3	<0.14
Category	AWF (dB)	Limits for E-Field Emissions (V/m) < 960MHz	Limits for H-Field Emissions (A/m) < 960 MHz
M1	0	631 - 1122	1.91 - 3.39
	-5	473.2 - 841.4	1.43 - 2.54
M2	0	354.8 - 631	1.07 - 1.91
	-5	266.1 - 473.2	0.8 - 1.43
M3	0	199.5 - 354.8	0.6 - 1.07
	-5	149.6 - 266.1	0.45 - 0.8
M4	0	<199.5	<0.6
	-5	<149.6	<0.45

Table.5.1. ANSI standards for HAC categories.

5.2 Method

A point of acoustic is marked on the PCB, which is usually 7mm away from the end of the PCB. RF emission ratings are based on the peak field strength as measured over a grid in the region of the ear piece. A measurement grid of 50x50 mm is centered over the acoustic output, at the height of 15mm. The grid is divided into nine cells and the robot controls the probe and moves the probe over the plane in a step size of approximately 5 mm for both the E field and H field. The highest field value is checked from the grid, the two values near to that one are deleted. Among the remaining field values, the maximum is taken as a final result. If the maximum value occurs at the center, than that value cannot be deleted. The E and H field values are required to be within limits as specified in the Table5.1 and categorized as M1, M2, M3 or M4, while the later is least immuned to HAC.

In simulation CST MWS is used to see the HAC results c.f Fig.5.1. Measurement is done on DAYS4 equipment c.f Fig.5.2.The antenna chassis combination is placed on a device holder and probe is moved over the scan area to measure the field strengths.

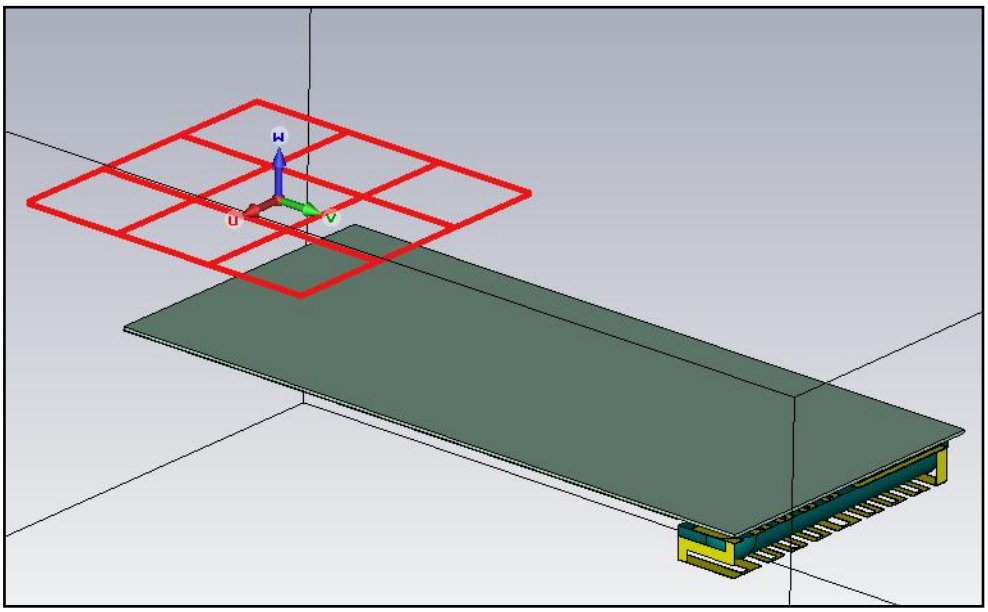

Fig.5.1.Simulation setup for HAC where a grid is placed at acoustic point away from antenna element.

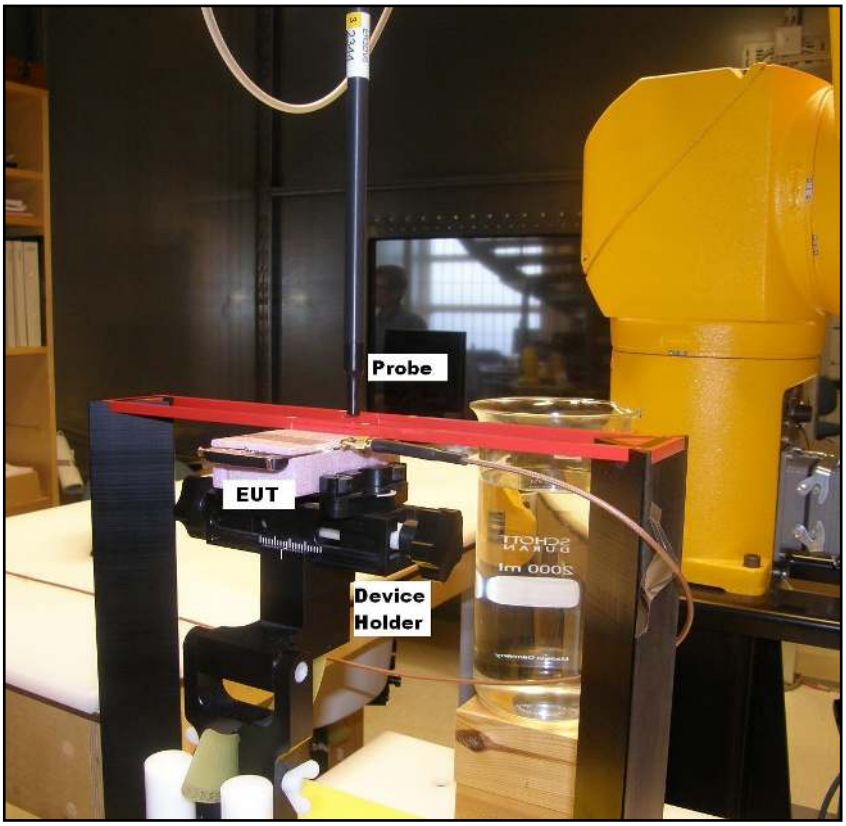

Fig.5.2.Measuremnet setup for HAC.

5.3 Simulated and Measured results

The loop antenna generates small excited surface currents on the system ground plane of the mobile phone because of its closed resonant path [26, 27].

For the loop antennas when the currents at the antenna feed and short are in the same direction it is called as common mode [26]. Fig 5.3 shows the near field distribution at the antenna and the acoustic point. The H field has a local maximum at the center of the chassis and E field exsist underneath the antenna element and at the end of the PCB see Fig.5.3 (a&c).

When the antenna is in balanced or differential mode the currents at feed and short point are in opposite direction as can be seen from Fig.5.3 (b). As a result the net current on the chassis reduces and leaves some cool areas at the end of the chassis.

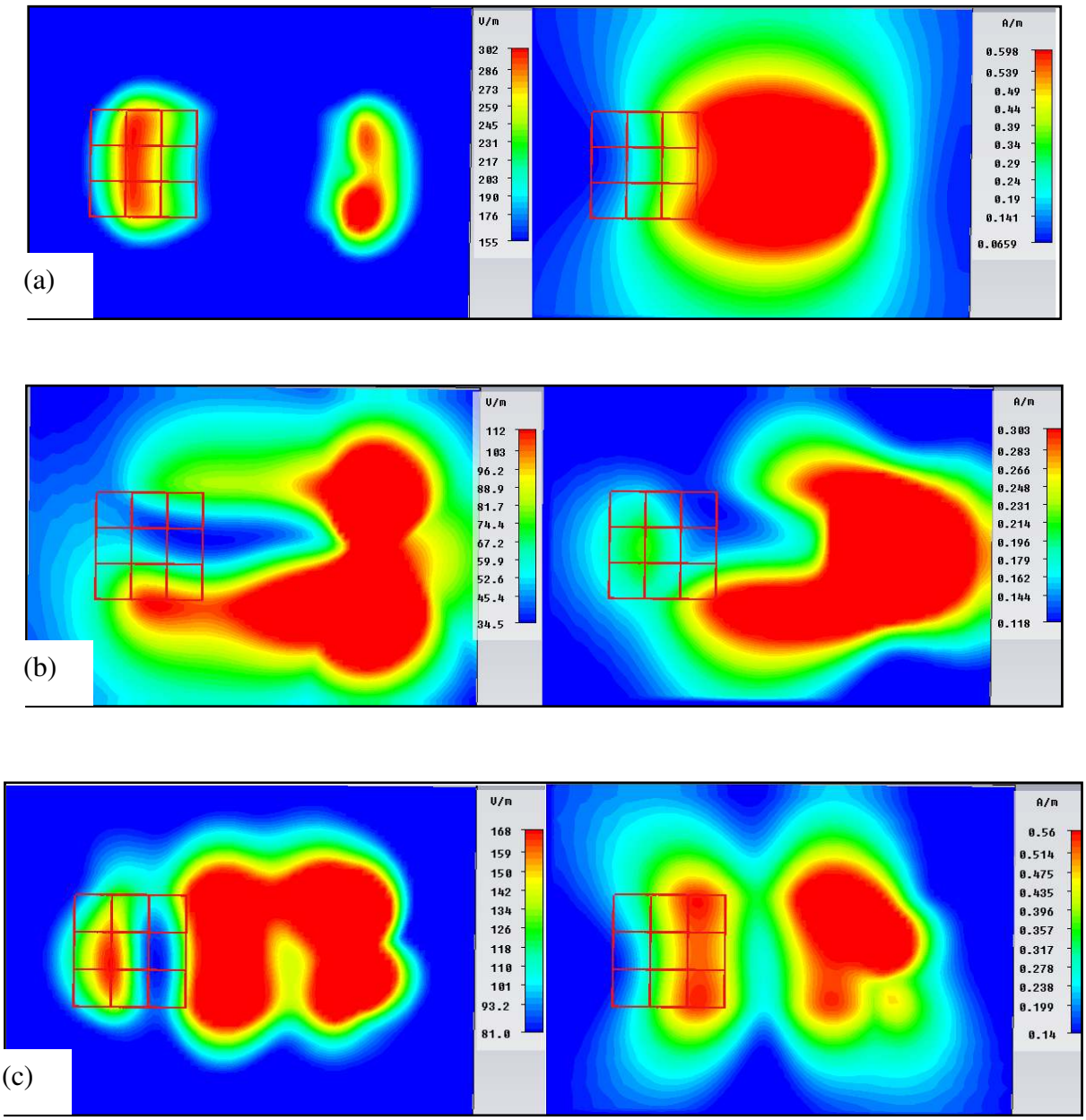

Fig.5.3 Simulated E field (right side) and H field (left side) at (a) 894MHz (b) 1740MHz and (c) 2600MHz.

During the measurement a signal of input power 0.25 W (24dBm), for the lower band and 0.125 W (21dBm) for the higher band, is used and following plots and field strengths are obtained see Fig.5.4.

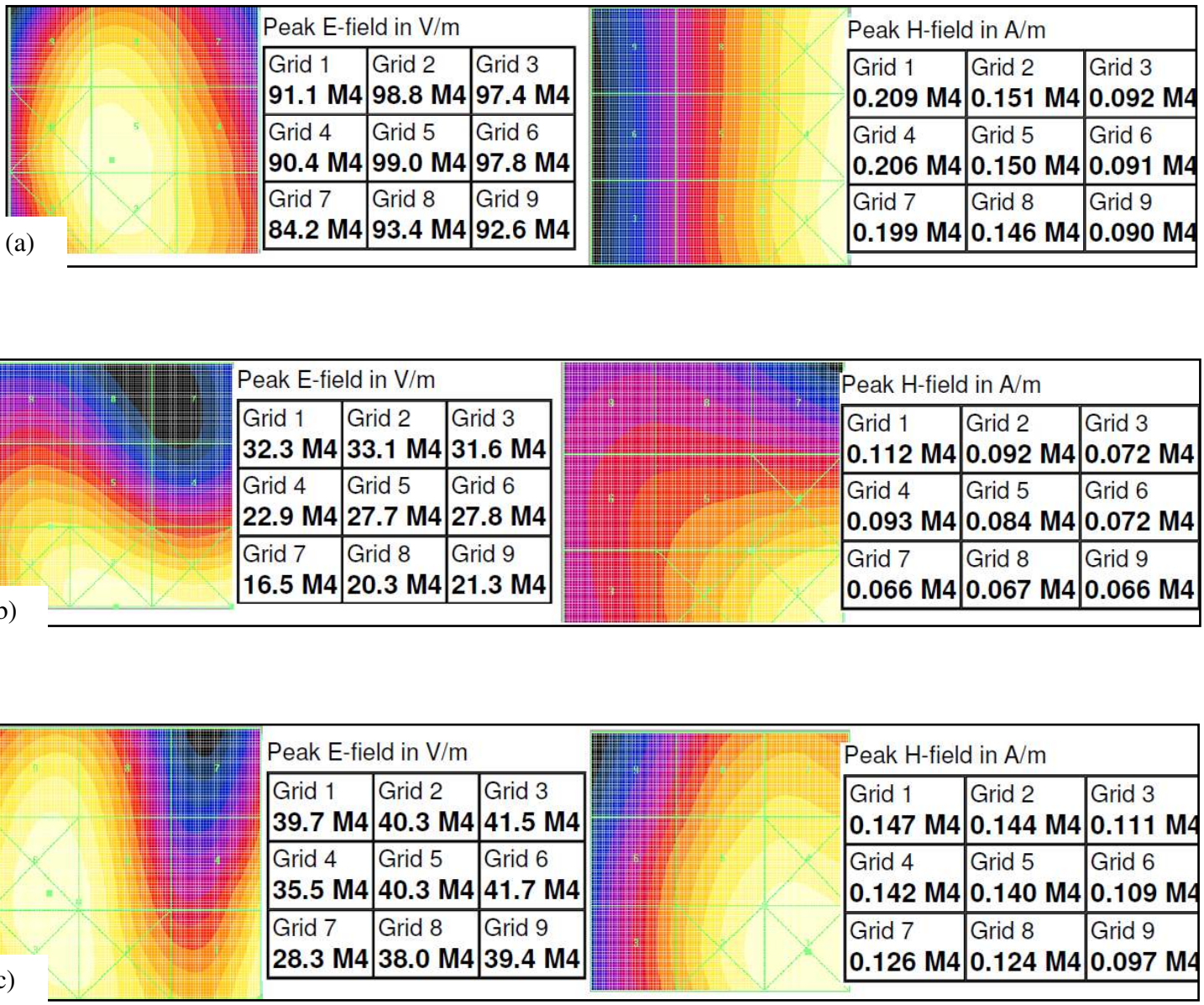

Fig.5.4 Measured E field (right side) and H field (left side) at (a) 894MHz (b) 1740MHz and (c) 1980MHz.

5.4 Conclusions

The measured results for the prototype antenna meets the HAC standard ANSI C63.19, as it generates very weak near field electric and magnetic fields because of its design. The reduction in the near fields in meander line antenna is due to its spatially distributed radiating sections.

It can also be inferred from the results that for the proposed antenna with a unbalanced feed against a ground chassis has a self-balanced mode, which is the differential mode, resulting in less currents induced on the ground plane [28].

CHAPTER: 6 DISCUSSIONS AND FUTURE WORK

6.1 Comparison with PIFA

A PIFA antenna already available in CST MWS examples is simulated c.f Fig.6.1, and is compared with the meanderline loop antenna with respect to the SAR and HAC performance. Details about SAR and HAC have already been explained in earlier chapters. A comparison is done in Table 6.1 and Table 6.2.

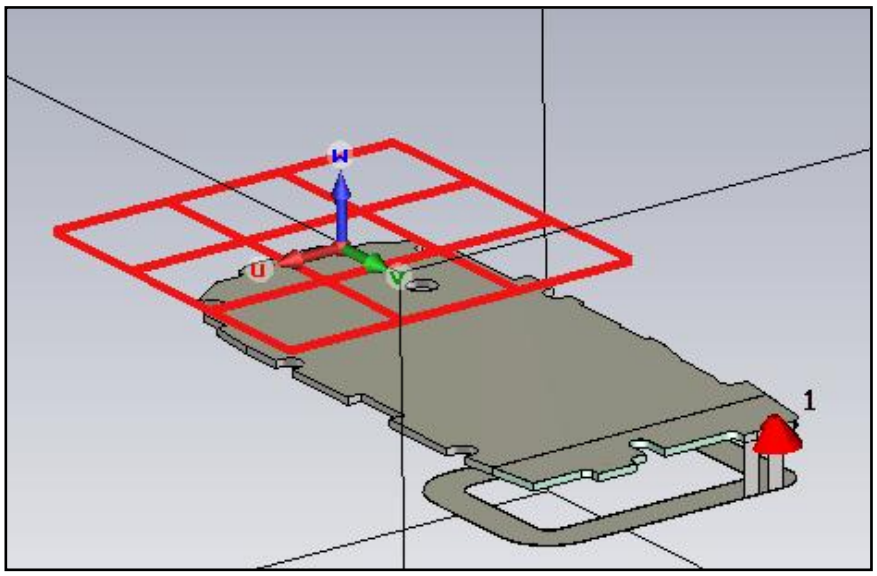

Fig.6.1 Simulation model of dual band PIFA antenna

Frequency (MHz)	SAR			
	PIFA		Proposed Antenna	
	10 g	1 g	10g	1g
900	1.36	1.98	0.89	1.29
1800	0.61	0.97	0.32	0.47

Table.6.1. Comparison of simulated SAR values for PIFA and proposed antenna.

Frequency (MHz)	HAC	
	PIFA	Proposed Antenna
900	M2	M4
1800	M2	M4

Table.6.2. Comparison of simulated HAC values for PIFA and proposed antenna.

This proposed design behavior owes that the excited currents on system ground plane are smaller than that of the conventional internal mobile phone antennas such as the PIFAs. System ground plane of the mobile phone plays an important role in the performances of the internal PIFA, especially the antenna's achievable operating bandwidth.

6.2 Future Work

The radiation efficiency measurements have shown that the antenna has a η less than -1.5 dB for 700 to 790MHz. The Q plot in Fig.6.2 shows the BW potential for 750MHz band. Switching can be done to make the antenna working for lower LTE US band. In simulations, passive matching is done to tune down the S11.Fig.6.3 (a) shows the schematic for the matching circuit and (b) shows the tuned S11. The switching is not yet practically implemented so there are no measured results to see the overall performance.

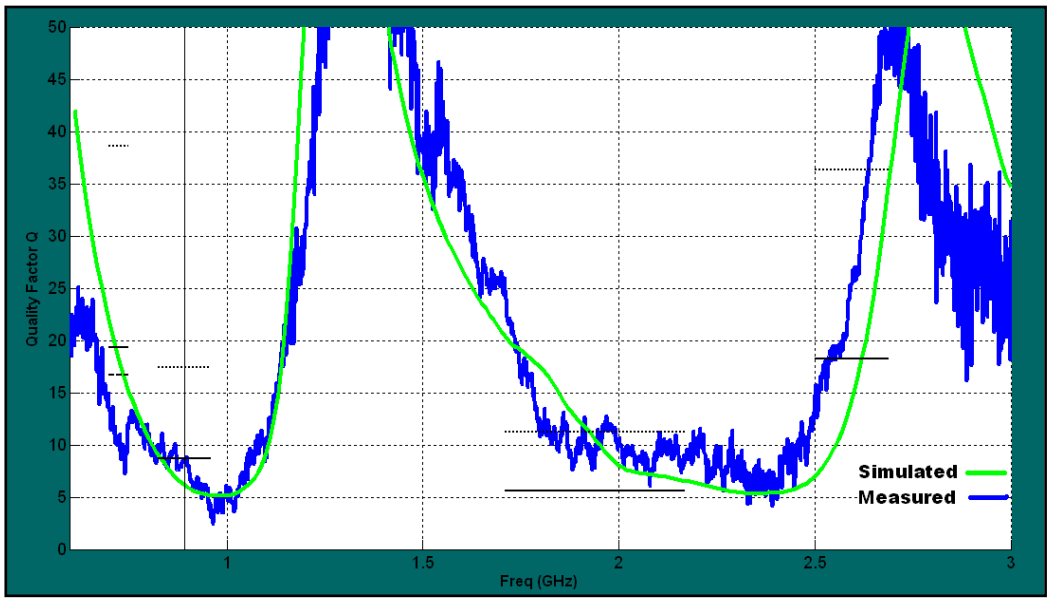

Fig.6.2. Q plot for simulated and measured response.

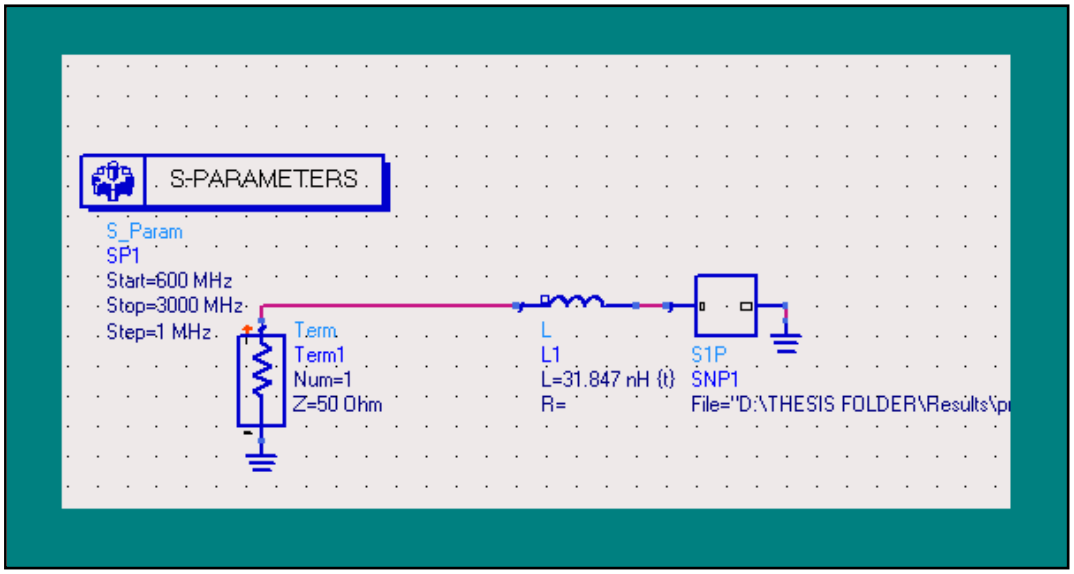

Fig.6.3 (a) Schematics for passive matching of antenna.

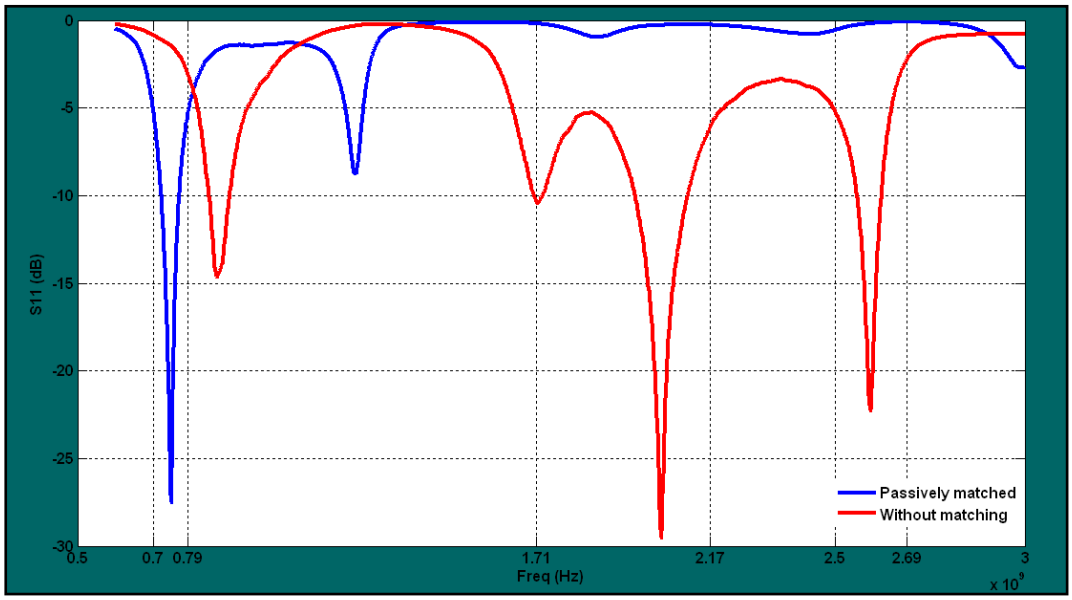

Fig.6.3 (b) S11 response for both passive matching and without matching.

The BW potential has been demonstrated (Q-simulation and simulated matching) so the implementation of an RF-switch needs to be investigated Also to check the influence of components on antenna performance, that are typically present in phones such as battery, speakers, display and jacks.

6.3 Conclusions

The concept of using a single loop as a cellular antenna in mobile phones has been studied. The newly proposed design for multiband internal antenna has a different radiating mechanism, as compared to the conventional PIFA. It has a longer electrical length so that it can provide lower concentration of surface current distribution. The folded and meandered structure has good impedance matching and has the ability to operate at multiple frequency bands simultaneously.

It is highly efficient in terms of small volumetric size for a given bandwidth of operations. It has little detuning in the high band in terms of body effects and has potential for 700MHz.

The different radiation modes have been analyzed regarding their order of resonances, current distribution on antenna structure and ground plane for balanced and unbalanced modes. The impact of body effects on the radiation efficiency has been quantified beside head and beside head with hand.

According to prototype measurements, SAR standards have been satisfied for all the frequencies. The measured results for the prototype antenna meet the HAC standard ANSI C63.19.

The design has been successfully implemented and the measured results are meeting the requirements of the proposed work.

Some of the future work is to investigate the implementation of an RF-switch, checking the influence of components that are typically present in phones such as battery, speakers, display, jacks etc.

REFERENCES

[1] Yun-Wen Chi and Kin-Lu Wong, "Small-Size Multiband Folded Loop Antenna for Small-Size Mobile Phone", presented at IEEE Antennas and Propagation Society International Symposium, San Diego, CA, Jul. 2008.

[2] Byung-kil Yu et al, "A folded and bent internal loop antenna for GSM/DCS/PCS operation of mobile handset applications", Microwave and optical technology letters , vol. 48, pp. 463-467, Mar. 2006.

[3] Yong-Sun Shin et al, "A compact multiband PIFA with the modified ground plane and shorting plate for wireless communication applications", Microwave and Optical Technology Letters, vol 50, Issue 1, pp. 114 – 117, 19 Nov. 2007.

[4] W. Geyi et al, "handset antenna design: practice and theory", Progress In Electromagnetics Research, PIER 80, 123–160, 2008.

[5] G. Wen et al, "Handset antenna design: practice and theory", Progress in Electromagnetics Research, vol 80, pp.123–160, 2008.

[6] "The challenges of handset antenna design", Roke Manor Research Ltd, Hampshire, 2005.

[7] R. Bancroft, "Fundamental dimension limits of antennas," unpublished paper, Westminster, Colorado.

[8] Kingsley, S., "Advances in handset antenna design", RF Design, May 2005.

[9] M. Gustafsson, "Bandwidth, Q Factor, And Resonance Models Of Antennas", Progress In Electromagnetics Research, PIER 62, pp.1–20, 2006.

[10] H. A. Wheeler, "Fundamental limitations of small antennas," Proc. IRE, pp. 1479-1484, Dec. 1947.

[11] Pertti Vainikainen, "Resonator-Based Analysis of the Combination of Mobile Handset Antenna and Chassis", IEEE transactions on antennas and propagation, vol. 50, No. 10, Oct. 2002.

[12] Arenas, J. J., "Balanced and single-ended handset antennas free space and human loading comparison," Microwave and Optical Technology Letter, Vol. 51, No. 9, pp. 2248-2254, Sep. 2009.

[13] Jonathan Ide et al, "Balanced-unbalanced antennas", USPTO Application #20090109104, Apr.30, 2009.

[14] O. Kivekäs, et al, “Bandwidth, SAR, and efficiency of internal mobile phone antennas”, IEEE Trans. on electromagnetic compatibility, vol. 46, pp. 71-86, Feb. 2004.

[15] Krzysztofik, W.J, “Meandered Double-PIFA Antenna – Handset / Human Interaction”, presented at Microwaves, Radar & Wireless Communications, May. 2006.

[16] Richard C. Hohnson, “Antenna Engineering Hand book, New York, McGraw Hill, 1993, Chapter 5.

[17] Mavridis, G.A, “Quality Factor Q of a Miniaturized Meander Microstrip Patch Antenna”, Proc. Antennas and Propagation Society International Symposium, San Diego, CA, pp. 1 – 4, July. 2008.

[18] Chun-I Lin and Kin-Lu Wong, “Internal Multiband Loop Antenna for GSM/DCS/PCS/UMTS Operation In The Small-Size Mobile Device”, Microwave and Optical Technology Letters, vol 50, Issue 5, pp 1279 – 1285, Mar.27, 2008

[19] A. G. Alhaddad et al, “Compact Dual-band Balanced Handset Antenna for WLAN Application”, PIERS ONLINE, vol. 6, NO. 1, pp. 11-15, 2010.

[20] Keisuke Noguchi, “Increasing the bandwidth of a small meander-line antenna consisting of two strips”, Electronics and Communications in Japan (Part II: Electronics), vol 83 Issue 10, pp 35 – 43, Aug.31, 2000.

[21] Aycan Erentok, “A Summary of Recent Developments on Metamaterial-based and Metamaterial-inspired Efficient Electrically Small Antennas”, Turkish Journal of Electrical Engineering & Computer Sciences, pp. 21-32, 2008.

[22] Salah I. Al-Mously et al , “A Study of the Hand-Hold Impact on the EM Interaction of a Cellular Handset and a Human”, World Academy of Science, Engineering and Technology, Vol. 28, April 2008.

[23] Pekka Halla, “Specific absorption rate design of 3rd generation handsets”, Masters thesis, Helsinki university of technology, 2008.

[24] Abd-Alhameed et al, “SAR and radiation performance of balanced and unbalanced mobile antennas using a hybrid formulation," IEE Proceedings-science, Measurement and Technology, Special Issue on Computational Electro- magnetic, Vol. 151, No. 6, 440-444, Nov. 2004.

[25] Yun-Wen Chi ,“Quarter-Wavelength Printed Loop Antenna With an Internal Printed Matching Circuit for GSM/ DCS/PCS/UMTS Operation in the Mobile Phone”, IEEE transactions on antennas and propagation, vol. 57, NO. 9, Sept, 2009.

[26] “IEEE American National Standard Methods of Measurement of Compatibility between Wireless Communication Devices and Hearing Aids”, IEEE ANSI C63.19-2007.

[27] Ping Hui ,“Near Fields of Phased Antennas for Mobile Phones”, Nokia Research Center , APMC Singapore, Dec. 2009.

[28] Wei-Yu Li, “Hearing Aid-Compatible Loop Chip Antenna for Penta-Band Clamshell Mobile Phone Application”, APMC Singapore, Dec. 2009

[29] S. Hayashida, H. Morishita and K. Fujimoto, “Self-balanced wideband folded loop antenna,” IEE Proc. Microwave antennas and propagation , vol. 153, pp. 7-12, Feb. 2006.